Natural rubber based films integrating Zosteric acid analogues as bioactive monomers

Thi Nguyet Tran, Pamela Pasetto, Christelle Pichon, David Bruant, Guillaume Brotons, Arnaud Nourry

▶ **To cite this version:**

Thi Nguyet Tran, Pamela Pasetto, Christelle Pichon, David Bruant, Guillaume Brotons, et al.. Natural rubber based films integrating Zosteric acid analogues as bioactive monomers. Reactive and Functional Polymers, 2019, 144, pp.104343. 10.1016/j.reactfunctpolym.2019.104343 . hal-02319523

HAL Id: hal-02319523
https://hal.science/hal-02319523

Submitted on 20 Jul 2022

HAL is a multi-disciplinary open access archive for the deposit and dissemination of scientific research documents, whether they are published or not. The documents may come from teaching and research institutions in France or abroad, or from public or private research centers.

L'archive ouverte pluridisciplinaire **HAL**, est destinée au dépôt et à la diffusion de documents scientifiques de niveau recherche, publiés ou non, émanant des établissements d'enseignement et de recherche français ou étrangers, des laboratoires publics ou privés.

Distributed under a Creative Commons Attribution - NonCommercial 4.0 International License

Version of Record: https://www.sciencedirect.com/science/article/pii/S1381514819302986
Manuscript_b7ae3f731c94094ecf1660afd67c8417

Natural Rubber based films integrating Zosteric acid analogues as bioactive monomers

Thi Nguyet Tran[1], Pamela Pasetto[1], Christelle Pichon[1], David Bruant[2], Guillaume Brotons[1], Arnaud Nourry[1,*]

[1] Institut des Molécules et Matériaux du Mans, UMR 6283 CNRS – Le Mans Université, Avenue Olivier Messiaen, 72085 Le Mans Cedex 9, France.

[2] Lycée Notre Dame, 23 Avenue François Mitterrand, 72000 Le Mans, France

Thi_Nguyet.Tran.Etu@univ-lemans.fr, Pamela.Pasetto@univ-lemans.fr, Christelle.Pichon@univ-lemans.fr, David.Bruant@ac-nantes.fr, Guillaume.Brotons@univ-lemans.fr,

* Corresponding autor Arnaud.Nourry@univ-lemans.fr

Abstract

This article describes the synthesis and the evaluation of the biological activity of antibacterial bio-based elastomeric materials. The synthesis strategy relies on the photo-copolymerization of macromonomers containing an isoprenic repeating unit (obtained from Natural Rubber) and original monomers designed from Zosteric Acid scaffold (known for its antifouling activity) and covalently bound to the polymer network. The materials were obtained as cross-linked thick films and were characterized by InfraRed Spectroscopy, contact angle, and thermal analyses. No significant release of any bioactive substance was observed after immersions in water, confirming the non-leaching property. Biological assays were carried out with five strains of pathogenic bacteria and three strains of marine bacteria and the results highlighted the antibacterial and fouling release properties of these novel promising materials.

Keywords (max 6)

Natural rubber, polyisoprene, antifouling materials, Zosteric acid, antibacterial polymers, antimicrobial films

Introduction

Biofouling or biocontamination is the colonization of a substrate by a range of micro- and macro-organisms and by their side-products[1-5]. It is recognized as a major problem for numerous applications such as biomedical implants and devices[6-8], biosensors, textiles[9], food packaging and storage, water purification systems[10, 11], industrial and marine equipment[12].

© 2019 published by Elsevier. This manuscript is made available under the CC BY NC user license
https://creativecommons.org/licenses/by-nc/4.0/

In the hospitals, pathogenic bacteria are a widespread problem since they form a well-defined bacterial network on the surfaces (named biofilm), which allows them to develop and acquire resistance to antibiotics, causing numerous infections and being one of the primary causes of death worldwide[13, 14]. The contamination is due to several sources such as the surgical acts; the patient's own skin or mucous membrane; a contaminated medical device or equipment; contact with family members, other patients or even air suspensions after surgery[15]. In marine or fresh water environment, biofilms start with the adhesion of molecules (proteins, inorganic compounds…) on the immerged objects followed by deposition of bacterial cells. This provokes the modification of the surface physicochemical properties[16], allowing microorganisms such as microalgae and macro organisms such as mussels and barnacles to adhere. The attachment of this biofilm on boat hulls can dramatically increase drag and therefore fuel consumption, causing a major issue in the marine industry[3, 17]. On water treatment devices, the accumulation of organisms damages their function[10], while the efficiency of immerged captors is reduced. Different strategies have been used to fight bacterial contamination and the preparation of bioactive polymeric materials is just one of these. Many antimicrobial polymers, polymer-based antimicrobial hydrogels and polymer-coated antimicrobial surfaces have been developed and are presented in recent reviews[18, 19]. Other formats such as polymeric nanoparticles[20, 21] or the use of natural or synthetic antibacterial polymers in the additive manufacturing (3D impression)[22] have been designed. As a result, in the recent past, great efforts have been invested to make functional polymeric devices or coatings possessing antimicrobial and/or antifouling properties that prevent biofilm formation and subsequent corrosion[23, 24]. However, an ideal solution has not been found yet. The harmful effects to human health and to the environment of several released biocides has been recognized; particularly, the ban of TBT (tributyltin) and other metal based paints in the market in 2003, due to their toxicities toward non-target organisms and the surrounding environment[25, 26]. In this context, the development of new solutions able to replace the presently dominating products is becoming imperative. One of the most promising alternatives is offered by the development of antifouling polymers in which the active substances are compounds naturally occurring in marine organisms and operating as natural anti-settlement agents [27, 28]. The great interest of these Natural Product Antifoulants (NPAs) for fouling control is through a non-toxic mechanism. Moreover, the use of petrochemicals as a starting material is disadvantageous since they are no-renewable resources. The price, the availability of petroleum and, in particular the society concerns over global climate change continue to create increasing market pressure on the industry and domestic use of petrochemicals. That is why a great alternative could be the incorporation of a less toxic natural antifouling compound on bio-based polymer networks, thus generating antifouling materials[29, 30].

The polymer network of this research work was made from natural rubber (NR) , which is an attractive bio-based elastomer due to its excellent properties such as high elasticity, mechanical strength, fatigue resistance, wide range of operating temperatures and tear strength together with environmental friendliness[31]. As natural rubber is constituted of polyisoprene chains with *cis*-1,4-carbon-carbon double bonds and a stereoregular configuration of the polymeric backbone, it is possible to chemically modify it to give other polymeric materials. Our group developed a *one pot* synthesis of Carbonyl Telechelic Natural Rubber oligomers

(CTNR) bearing an aldehyde and a ketone chain ends *via* the controlled degradation of NR by using periodic acid [32-34].

Zosteric acid or *p*-(sulfoxy) cinnamic acid (ZA, Figure 1) is a natural product isolated from the seagrass *Zostera marina*[35] displaying an antibiofouling activity (against bacteria and barnacles)[36-40]. In addition to its natural origin, ZA has a very low toxicity (EC_{50} ~170-450 ppm)[38, 41, 42]. The mode of ZA antifouling action has not been fully elucidated yet, however, it was supposed that ZA could act as an environmental cue, leading to a global stress on the cells and favoring the expression of various proteins necessary to escape from adverse conditions[37, 43]. It was recently proposed that ZA might be a storage compound that is enzymatically converted to coumaric acid by sulfatase enzymes when environmental stress is present[44, 45]. The chemical structure of ZA (Figure 1) contains a sulfate phenolic ester group at one end and a carboxylic acid group conjugated to a double bond (*E* configuration) at the other end (*para* position). In fact, the antifouling efficiency of ZA was firstly reported to be associated with the sulfate ester group by Todd *et al*.[35] They demonstrated that in general synthetic sulfate esters have similar antifouling (AF) properties. Indeed, non-sulfated phenolic acids were ineffective even at concentration 60-fold higher than the EC_{50} of sulfate esters. Later, Villa *et al.*[38] showed for the first time that the AF activity of ZA may be also due to the carboxylic group according to the types of bacteria. For instance, methyl zosterate was inactive against *C. albicans*, while had antiadhesive effects on *Staphylococcus aureus*. Guzman *et al*. [46] pointed out that the natural phenol *para*-coumaric acid (CA) provided more potent bacterial growth inhibition compared to ZA and cinnamic acid, becoming an interesting scaffold for the development of new antimicrobial compounds (Figure 1). Successively, a study published in 2015[44, 45] questioned certain conclusions of the structure-activity relationship. Indeed, the authors followed the sample preparation methods described in the literature in order to synthesize Zosteric acid or its salts. They showed that some traces of CA were still present in most of the synthesized ZA compounds. According to them, the activity associated with Zosteric acid was in fact linked to the presence of these impurities. This hypothesis was recently confirmed by C. Cattò *et al.*[42] when they studied the structure-activity relationships of ZA analogs. Several modifications based on ZA-scaffold were performed: the substitutions of the aromatic ring, the modifications of the alkene or the carboxylic acid. A library of 43-molecules was tested for antifouling activity against *E. coli.* They demonstrated that the presence of the sulfate function was not necessary because CA was more active than ZA itself. The presence of the carboxylic acid (-COOH) was also important because if this acid is esterified (methyl or ethyl) or replaced by other functional groups such as an aldehyde or an alcohol, the biological activity also generally failed. Nevertheless, the presence of a hydroxyl group in the para position of the ring allowed maintaining an interesting activity with some esters. The replacement of a saturated alkyl chain or *Z*-configuration in place of the double bond showed a loss of antifouling activity, confirming that it was highly necessary to have an alkene with the *E*-configuration, conjugated with RCOOH group for the generation of an antifouling activity.

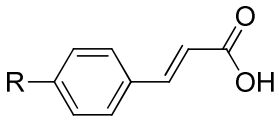

R = OSO_3H: Zosteric Acid (ZA)
R = OH: *para*-Coumaric Acid (CA)
R = H: cinnamic acid

Figure 1: Chemical structure of Zosteric Acid, para-Coumaric Acid and Cinnamic Acid.

In a previous work of our team, it was showed that natural rubber based coatings without bioactive compounds presented a low but detectable antifouling activity against marine and pathogenic bacteria[47]. These antifouling/antibacterial activities against two species of pathogenic bacteria *(Pseudomonas aeruginosa, Staphylococcus aureus)* were increased by the incorporation of the Zosteric Acid (ZA) or its salt (as powders) in the polyisoprene matrix[48]. In this first work, ZA was just blended to the prepolymerization mixture, which means that ZA was not covalently linked to the polymer network and so it could be released into the environment. To tackle this problem, this paper will focus on developing a new ecofriendly bio-based antibacterial/antifouling material by covalently integrating new Zosteric acid derivates (Figure 1) in the natural rubber network by photopolymerization. The results obtained so far concerning the optimization of the films formulation, the assessment of the non-leaching properties and the action against five strains of the most dangerous pathogenic bacteria (*Pseudomonas aeruginosa*, *Staphylococcus aureus*, *Staphylococcus epidermidis, Bacillus subtilis and Escherichia coli*) and three strains of marine bacteria (*Flavobacterium, Bacillus, Alteromonas*) will be presented.

1 Experimental Section

1.1 Materials

Natural rubber (NR, STR5LCV60) was produced by Jana Concentrated Latex Co., Songkhla, Thailand. Periodic acid (H_5IO_6, ≥99%), triethylamine (Et_3N, ≥ 99.0%), acryloyl chloride (≥ 97.0%), 2-hydroxy-2-methyl-1-phenyl-propan-1-one (Darocur 1173, ≥ 97.0%), Pentaerythritol A, technical grade), *tert*-Butyl(triphenylphosphoranylidene)acetate, mesyl chloride, anhydrous dimethylformamide (DMF), dimethylsulfoxide (DMSO) were purchased from Sigma Aldrich and used without any further purification. Trifluoroacetic acid was purchased from Alfa Aesar. Sodium borohydride ($NaBH_4$, ≥ 98%), *tert*-Butyldimethylsilyl chloride (≥ 98%) were purchased from Acros Organics. *Tetra-n*-butylammonium fluoride, Acetic acid, triphenylphosphine, 4-hydroxybenzaldehyde, 4-hydroxybutylacrylate, diisopropylazido-dicarboxylate (DIAD), sodium bicarbonate ($NaHCO_3$) technical reagent grade, potassium carbonate, lithine (LiOH), anhydrous magnesium sulfate laboratory reagent grade, sodium thiosulfate pentahydrate ($Na_2S_2O_3.5H_2O$) and sodium chloride general purpose grade were purchased from Fisher Scientific. Dichloromethane (DCM), tetrahydrofuran (THF) were purchased from Aldrich and dried in a dry

solvent station GT S100 (Glass Technology). Ethyl acetate (EtOAc) and cyclohexane were purchased from Fisher Scientific and used after distillation. Water was deionized using Ultrapure Milli-Q Reagent Water System Millipore and used at 18MΩ. Concentrated HCl and NaOH solutions (research grade, Aldrich Chem. Co.) were diluted to obtain the desired concentrations.

1.2 Physico-Chemical Characterization

1.2.1 Nuclear magnetic resonance (NMR) Analysis

^{1}H-NMR and ^{13}C-NMR spectra were respectively recorded at 400 and 100.6 MHz on a Bruker® spectrometer. The samples were dissolved in chloroform-*d* ($CDCl_3$) or methanol-d_4 (CD_3OD). The chemical shifts (δ) are expressed in part per million (ppm) relative to Me_4Si and the coupling constants (J) in Hertz.

1.2.2 Size Exclusion Chromatography Analysis

Number-average molecular weight ($\overline{M}_n$) and dispersity (Đ) were measured by size exclusion chromatography (SEC) in THF as eluent (flow 1 mL/min), at 35ºC, on a Waters® chain 2707 autosampler equipped with a 1515 Isocratic Pump and a guard column (Styragel 30x4.6 mm) connected to a column (Styragel HR2 + HR4, 300x7.8nm). The Waters® 2996 PDA and Waters® 2414 Refractive Index Detector were used. Calibration was performed with polystyrene (PS) standards in the range from 580 g/mol to 483000 g/mol. The molecular weights of the oligoisoprenes were corrected according to the Benoit factor equal to 0.67. Generally, the molecular weight of all oligomers was determined by SEC and by ^{1}H-NMR.

1.2.3 Liquid chromatography coupled to mass spectrometry (LC-MS) Analysis

Liquid chromatography coupled to mass spectrometry experiments were performed using an UltiMate™ 3000 Rapid Separation Binary System (Thermo Fischer Scientific), interfaced with a mass spectrometer MicroTOF-QIII (Bruker®), equipped with an electrospray-ionization source operating in the positive and negative mode. The spectra were recorded in the range scan of 50 to 1000 m/z. Chromatographic separations were performed using a C18 HTec (2.0x250mm inner diameter, 5µm particle size, Fischer Scientific) at a column temperature of 35°C and at a flow rate of 0.3 mL/min. The mobile phase composition was a mixture of water and acetonitrile with gradient time period.

1.2.4 Photopolymerization equipment

The samples used for the biological tests were polymerized using a UV-curing equipment (UV Fusion System Corporation, Hanau, Germany), equipped with a hydrogen lamp (power 120 Watt/cm). The belt speed was 1.6 m/min, and the light intensity 2.5W/cm^2. The pre-polymerization mixture was deposited in Teflon molds of 1 cm diameter and 0.5 mm depth and flexible disks were obtained after irradiation. The kinetic study of photopolymerization was carried out irradiating with a UV lamp in the wavelength range

320-390 nm. The light intensity was measured with a UV Power Meters, series C6080, and varied in the range 0.3-11mW/cm^2.

1.2.5 Fourier-Transform Infrared Spectroscopy (FTIR)

The photo-crosslinking reaction kinetic was monitored by a FTIR Vertex 70V Bruker spectrometer with a deuterated triglycine sulfate detector. The absorption bands were recorded in the range of 400 – 4000 cm $^{-1}$ with 16 scans and a resolution of 2 cm $^{-1}$. The data were analyzed using OPUS software. The conversion of functional groups at time (t) is denoted as % and it is defined by the equation **(1)**[49]

$$\% = \frac{\left(\frac{A1405}{A1375}\right)0-\left(\frac{A1405}{A1375}\right)t}{\left(\frac{A1405}{A1375}\right)0} * 100 \quad \textbf{(1)}$$

The areas under the absorbance peaks were calculated and reported at the initial time (A_0) and at different times (A_t). 1405 cm^{-1} corresponds to the $\delta_{=CH2}$ of the acrylate chains ends and 1375 cm^{-1} is the reference band which belongs to the δ_{-CH3} of the *cis*-1,4-polyisoprene repeating unit.

1.2.6 Microscopy

Scanning Electron Microscope: Micrographs were taken using a JEOL, JSM 6510 LV instrument. The samples were covered by a golden film before examination. Optical microscope: Zeiss scope A.1, equipped with a HB100 lamp. Axiovision program for images.

1.2.7 Themogravimetric analysis

Thermogravimetric analysis (TGA) was performed on a TA Instrument (Hi-Res-Dynamic TGA Q 500) with a heating rate 10ºC/min, under nitrogen or oxygen, in the range 25°C-800°C. The sample weight was 10 mg.

1.2.8 Contact Angle Measurement

Water contact angles (CAs) of sessile drops deposited on the samples surfaces were measured at room temperature using a homemade setup with halogen source and telecentric optics on the source and camera pathways. The thick polymer films obtained were deposited on glass slides that were first washed with ethanol and dried under strong filtered airflow. Contact angles were measured with a precision of 0.1°. At least 3 drops of 2 µL (with drop radius well below the water capillary length) were deposited on separated regions over the films surface to obtain an average value for each sample.

1.3 Synthesis of Monomers

1.3.1 Synthesis of Monomer (1)

*1.3.1.1 Preparation of (E) 3-(4-tert-butyldimethylsiloxy)phenyl acrylic acid **3**[50]*

To a solution of *p*-coumaric acid (5.000 g, 30.45 mmol, 1.0 equiv.) and imidazole (5.188 g, 76.13 mmol, 2.5 equiv.) in dry DMF (25 mL) was added under N_2 and at 0°C the TBSCl (11.47 g, 76.13 mmol, 2.5 equiv.). The reaction mixture was stirred at RT for 3 h then poured into distilled water (125 mL). The

cloudy solution was extracted with EtOAc (3*125 mL) and the combined organic layers were washed with brine (125 mL), dried over $MgSO_4$ and concentrated under vacuum. The residue was dissolved in THF/water (100/25 mL) and LiOH (729 mg, 30.45 mmol, 1.0 equiv.) was added. The reaction mixture was stirred at RT for 30 minutes and quenched by the addition of an HCl aqueous solution (1N) up to pH = 5. The aqueous layer was extracted with EtOAc (2*125 mL) and the combined organic layers were washed with brine (70 mL), dried over $MgSO_4$ and concentrated under vacuum. The residue was purified by chromatography on silicagel (cyclohexane / EtOAc 9:1 toward 0/1) to provide **3** (8.080 g, 29.02 mmol, 95%) as a white solid.

^{1}H NMR (200 MHz, $CDCl_3$) δ: 7.75 (d, J_{H3-H2} = 15.9 Hz, 1H, H-3), 7.45 (d, J_{H5-H6} = 8.6 Hz, 2H, H-5, H-9), 6.85 (d, J_{H6-H5} = 8.6 Hz, 2H, H-6, H-8), 6.32 (d, J_{H2-H3} = 15.9 Hz, 1H, H-2), 0.99 (s, 9H, *t*Bu), 0.23 (s, 6H, 2*Me).

*1.3.1.2 Preparation of 4-(acryloxy)butyl(E)-3(4-((tert-butyldimethylsilyl)oxy)phenyl)acrylate **4***

To a solution of 4-hydroxybutyl acrylate **4** (1.00 g, 6.93 mmol, 1.0 equiv.), protected *p*-coumaric acid **3** (3.87 g, 13.9 mmol, 2.0 equiv.), and PPh_3 (3.69 g, 13.9 mmol, 2.0 equiv.) in dry THF (110 mL), was added a solution of DIAD (2.7 mL, 2.81 g, 13.9 mmol, 2.0 equiv.) in dry THF (27 mL) under N_2 and at RT. The reaction mixture was stirred at RT for 3 days then concentrated under vacuum. The residue was purified by chromatography on silicagel (cyclohexane / EtOAc 95:5 toward 8/2) to provide **4** (2.396 g, 5.92 mmol, 85%) as a colorless oil.

^{1}H NMR (400 MHz, $CDCl_3$) δ: 7.63 (d, J_{H10-H9} = 16.0 Hz, 1H, H-10), 7.42 (d, $J_{H12-H13}$ = 8.5 Hz, 2H, H-12, H-16), 6.84 (d, $J_{H13-H12}$ = 8.5 Hz, 2H, H-13, H-15), 6.41 (dd, $J_{H1'-H1}$ = 1.5 Hz, $J_{H1'-H2}$ = 17.3 Hz, 1H, H-1'), 6.30 (d, J_{H9-H10} = 16.0 Hz, 1H, H-9), 6.13 (dd, J_{H2-H1} = 10.4 Hz, $J_{H2-H1'}$ = 17.3 Hz, 1H, H-2), 5.83 (dd, $J_{H1-H1'}$ = 1.5 Hz, J_{H1-H2} = 10.4 Hz, 1H, H-1), 4.25-4.21 (m, 4H, H-7, H-4), 1.83-1.79 (m, 4H, H-6, H-5) 0.98 (s, 9H, *t*Bu), 0.23 (s, 6H, 2*Me).

^{13}C NMR (100 MHz, $CDCl_3$) δ: 167.3 (C-3 or C-8), 166.2 (C-3 or C-8), 157.8 (C-14), 144.5 (C-10), 130.7 (C-1), 129.6 (C-12, C-16), 128.4 (C-2), 127.7 (C-11), 120.5 (C-13, C-15), 115.6 (C-9), 64.1 (C-4 or C-7), 63.8 (C-4 or C-7), 25.6 ((CH_3)$_3$C), 25.5 (C-5 or C-6), 25.4 (C-5 or C-6), 18.2 ((CH_3)$_3$*C*), -4.4 (2**C*H$_3$).

HRMS (ESI) $[M+Na]^+$ calculated for $C_{22}H_{32}NaO_5Si$: 427.1911, found: 427.1908.

*1.3.1.3 Preparation of 4-(acryloxy)butyl (E)-3-(4-hydroxyphenyl)acrylate (Monomer **1**)*

To a solution of **3** (940 mg, 2.32 mmol, 1.0 equiv.) in dry THF (17.5 mL), were added under N_2 and at RT, glacial acetic acid (0.95mL) and TBAF (solution in THF (1M), 6.96 mmol, 3.0 equiv., 7.0 mL). The reaction mixture was stirred at RT for 18h then THF was evaporated under vacuum. The residue was taken up in DCM (50 mL) and washed with a NaCl saturated aqueous solution (20 mL), then concentrated under vacuum. The organic layer was dried over $MgSO_4$ then concentrated under vacuum. The residue was purified by chromatography on silicagel (cyclohexane / EtOAc 4:1 toward 1/1) to provide **6** (627 mg, 2.16 mmol, 93%) as a colorless oil which crystallizes at room temperature.

^{1}H NMR (400 MHz, $CDCl_3$) δ: 7.63 (d, J_{H10-H9} = 16.0 Hz, 1H, H-10), 7.42 (d, $J_{H12-H13}$ = 8.6 Hz, 2H, H-12, H-16), 6.86 (d, $J_{H13-H12}$ = 8.6 Hz, 2H, H-13, H-15), 6.55 (bs, 1H, OH), 6.42 (dd, $J_{H1'-H1}$ = 1.4 Hz, $J_{H1'-H2}$ = 17.3 Hz, 1H, H-1'), 6.29 (d, J_{H9-H10} = 16.0 Hz, 1H, H-9), 6.13 (dd, J_{H2-H1} = 10.3 Hz, $J_{H2-H1'}$ = 17.4 Hz,

1H, H-2), 5.84 (dd, $J_{H1-H1'}$ = 1.4 Hz, J_{H1-H2} = 10.3 Hz, 1H, H-1), 4.26-4.22 (m, 4H, H-7, H-4), 1.83-1.80 (m, 4H, H-6, H-5).

^{13}C NMR (100 MHz, $CDCl_3$) δ: 167.8 (C-3 or C-8), 166.6 (C-3 or C-8), 158.3 (C-14), 145.0 (C-9), 131.0 (C-1), 130.0 (C-12, C-16), 128.3 (C-2), 126.8 (C-11), 115.9 (C-13, C-15), 115.0 (C-10), 64.2 (C-4 or C-7), 64.0 (C-4 or C-7), 25.4 (C-5 or C-6), 25.3 (C-5 or C-6).

IR (ATR, cm^{-1}): 3371, 2961, 2875, 1699, 1633, 1601, 1517, 1441, 1412, 1325, 1309, 1278, 1197, 1164, 965, 843, 812.

HRMS (ESI) $[M+Na]^+$ calculated for $C_{16}H_{18}NaO_5$: 313.1046, found: 313.1048.

1.3.2 Synthesis of Monomer (2)

1.3.2.1 Preparation of compound 4-((methylsulfonyl)oxy)butyl acrylate 7

To a solution of 4-hydroxybutyl acrylate (5.0 g, 34.7 mmol, 1.0 equiv.) in dry THF (7 mL) were added under N_2 and at 0°C triethylamine (9.7 mL, 69.4 mmol, 2.0 equiv.) and mesyl chloride (7.95 g, 69.4 mmol, 2.0 equiv.). The reaction mixture was stirred at RT for 2h then quenched by addition of distilled water (50 mL). The aqueous layer was extracted twice with EtOAc (2*100 mL). The combined organic layers were washed successively with NaCl aqueous saturated solution (200 mL), dried over $MgSO_4$ then concentrated under vacuum. The residue was purified by chromatography on silicagel (CH_2Cl_2 / EtOAc 1:0 toward 2/1) to provide **7** (7.685 g, 34.6 mmol, 99%) as a slightly brown oil.

^{1}H-RMN (400 MHz, $CDCl_3$), δ (ppm): 6.42 (dd, $J_{H1'-H1}$ = 1.4 Hz, $J_{H1'-H2}$ = 17.3 Hz, 1H, H-1'), 6.12 (dd, J_{H2-H1} = 10.4 Hz, $J_{H2-H1'}$ = 17.3 Hz, 1H, H-2), 5.85 (dd, $J_{H1-H1'}$ = 1.4 Hz, J_{H1-H2} = 10.4 Hz, 1H, H-1), 4.28 (t, J_{H4-H5} = 6.1 Hz, 2H, H-4), 4.21 (t, J_{H7-H6} = 5.9 Hz, 2H, H-7), 3.02 (s, 3H, H-8), 1.91-1.79 (m, 4H, H-5 H-6).

^{13}C-RMN (100 MHz, $CDCl_3$), δ (ppm): 166.0 (C-3), 130.6 (C-1), 128.3 (C-2), 69.2 (C-7), 63.4 (C-4), 37.2 (C-8), 25.6 (C-5 ou C-6), 25.2 (C-5 ou C-6).

1.3.2.2 Preparation of precursor 4-(4-formylphenoxy)butyl acrylate 6

To a solution of **7** (7.50 g, 33.4 mmol, 1.0 equiv.) in dry DMF (152 mL) were added under N_2 the *p*-hydroxybenzaldehyde (4.84 g, 39.7 mmol, 1.19 equiv.) and potassium carbonate (27.19 g, 197 mmol, 5.89 equiv.). The reaction mixture was stirred at 60°C for 16h then after cooling down, quenched by addition of distilled water (300 mL). The aqueous layer was extracted twice with EtOAc (2*200 mL). The combined organic layers were washed successively with a $NaHCO_3$ aqueous solution (200 mL) and an aqueous NaCl saturated solution (200 mL), dried over $MgSO_4$ then concentrated under vacuum to provide **6** (7.81 g, 31.46 mmol, 94%) as a colorless oil.

^{1}H-RMN (200 MHz, $CDCl_3$), δ (ppm) : 9.86 (s, 1H, CHO), 7.84 (d, $J_{H10\,H9}$ = 8.8 Hz, 2H, H-10 H-12), 7.00 (d, $J_{H9\ H10}$ = 8.8 Hz, 2H, H-9 H-13), 6.42 (dd, $J_{H1'-H1}$ = 1.7 Hz, $J_{H1'-H2}$ = 17.2 Hz, 1H, H-1'), 6.12 (dd, J_{H2-H1} = 10.3 Hz, $J_{H2-H1'}$ = 17.2 Hz, 1H, H-2), 5.84 (dd, $J_{H1-H1'}$ = 1.7 Hz, J_{H1-H2} = 10.2 Hz, 1H, H-1), 4.25 (t, J_{H4-H5} = 6.1 Hz, 2H, H-4), 4.09 (t, J_{H7-H6} = 5.9 Hz, 2H, H-7), 1.96-1.87 (m, 4H, H-5 H-6).

^{13}C-RMN (100 MHz, $CDCl_3$), δ: (ppm) 190.6 (CHO), 166.0 (C-3), 163.8 (C-8), 131.8 (C-10, C-12), 130.6 (C-1), 129.8 (C-11), 128.3 (C-2), 114.6 (C-9, C-13), 67.5 (C-7), 63.9 (C-4), 25.6 (C-5 ou C-6), 25.2 (C-5 ou C-6).

1.3.2.3 Preparation of compound (E)-3-(4-(4-(acryloxy)butyloxy)phenyl) acrylic acid terbutyl ester 8

To a solution of **6** (1.213 g, 4.89 mmol, 1.0 equiv.) in dry DCM (28 mL) was added under N_2 at RT *t*-Bu-2-triphenylphosphoranylideneacetate (2.39 g, 6.36 mmol, 1.3 equiv.). The reaction mixture was stirred at RT for 24h then quenched by addition of distilled water (20 mL). Phases were separated and the organic layer was washed with brine (40 mL). Aqueous layers were extracted once with DCM (50 mL). Combined organic layers were dried over $MgSO_4$ then concentrated under vacuum. The residue was purified by chromatography on silicagel (cyclohexane / EtOAc 4:1) to provide **8** (1.326 g, 3.83 mmol, 78%) as a colorless oil.

^{1}H-RMN (400 MHz, $CDCl_3$), δ (ppm) : 7.54 (d, $J_{H14\text{-}H15}$ = 15.9 Hz, 1H, H-14)), 7.44 (d, $J_{H10\ H9}$ = 8.7 Hz, 2H, H-10 H-12), 6.87 (d, $J_{H9\ H10}$ = 8.7 Hz, 2H, H-9 H-13), 6.40 (dd, $J_{H1'\text{-}H1}$ = 1.5 Hz, $J_{H1'\text{-}H2}$ = 17.3 Hz, 1H, H-1'), 6.24 (d, $J_{H15\text{-}H14,}$ = 15.9 Hz, 1H, H-15), 6.12 (dd, $J_{H2\text{-}H1}$ = 10.4 Hz, $J_{H2\text{-}H1'}$ = 17.3 Hz, 1H, H-2), 5.82 (dd, $J_{H1\text{-}H1'}$ = 1.5 Hz, $J_{H1\text{-}H2}$ = 10.4 Hz, 1H, H-1), 4.24 (t, $J_{H4\text{-}H5}$ = 6.1 Hz, 2H, H-4), 4.02 (t, $J_{H7\text{-}H6}$ = 5.8 Hz, 2H, H-7), 1.91-1.85 (m, 4H, H-5 H-6), 1.53 (s, 9H, *t*Bu).

^{13}C-RMN (100 MHz, $CDCl_3$), δ: (ppm) 166.6 (C-16), 166.1 (C-3), 160.4 (C-8), 143.1 (C-14), 130.6 (C-1), 129.5 (C-10, C-12), 128.4 (C-2), 127.3 (C-11), 117.6 (C-15), 114.7 (C-9, C-13), 80.1 ($(CH_3)_3C$), 67.3 (C-7), 64.0 (C-4), 28.2 ($(CH_3)_3C$), 25.7 (C-5 ou C-6), 25.3 (C-5 ou C-6).

HRMS (ESI) $[M+Na]^+$ calculated for $C_{20}H_{26}NaO_5$: 369.1672, found: 369.1665.

*1.3.2.4 Preparation of (E)-3-(4-(4-(acryloxy)butyloxy)phenyl) acrylic acid (Monomer **2**)*

To a solution of **8** (1.288 g, 3.72 mmol, 1.0 equiv.) in dry DCM (20 mL) was added under N_2 at RT, TFA (0.28 mL, 3.46 mmol, 10 equiv.). The reaction mixture was stirred at RT for 1h (monitored by TLC) then concentrated under vacuum. The residue was purified by chromatography on silicagel (Cyclohexane / EtOAc 1:1 toward 0/1) to provide **2** (959 mg, 3.30 mmol, 89%) as a white solid.

^{1}H-RMN (400 MHz, $CDCl_3$), δ (ppm) : 7.74 (d, $J_{H14\text{-}H15}$ = 15.9 Hz, 1H, H-14)), 7.50 (d, $J_{H10\ H9}$ = 8.8 Hz, 2H, H-10 H-12), 6.90 (d, $J_{H9\ H10}$ = 8.8 Hz, 2H, H-9 H-13), 6.41 (dd, $J_{H1'\text{-}H1}$ = 1.5 Hz, $J_{H1'\text{-}H2}$ = 17.3 Hz, 1H, H-1'), 6.32 (d, $J_{H15\text{-}H14,}$ = 15.9 Hz, 1H, H-15), 6.12 (dd, $J_{H2\text{-}H1}$ = 10.4 Hz, $J_{H2\text{-}H1'}$ = 17.3 Hz, 1H, H-2), 5.83 (dd, $J_{H1\text{-}H1'}$ = 1.5 Hz, $J_{H1\text{-}H2}$ = 10.4 Hz, 1H, H-1), 4.25 (t, $J_{H4\text{-}H5}$ = 6.1 Hz, 2H, H-4), 4.04 (t, $J_{H7\text{-}H6}$ = 5.8 Hz, 2H, H-7), 1.93-1.86 (m, 4H, H-5 H-6),

^{13}C-RMN (100 MHz, $CDCl_3$), δ: (ppm) 172.5 (C-16), 166.2 (C-3), 161.1 (C-8), 146.7 (C-14), 130.7 (C-1), 130.1 (C-10, C-12), 128.4 (C-2), 126.8 (C-11), 114.9 (C-9, C-13), 114.6 (C15), 67.4 (C-7), 64.1 (C-4), 25.8 (C-5 ou C-6), 25.4 (C-5 ou C-6).

IR (ATR, cm^{-1}): 2946, 2873, 1718, 1673, 1628, 1601, 1574, 1508, 1440, 1408, 1300, 1287, 1193, 972, 825, 810.

HRMS (ESI) $[M+Na]^+$ calculated for $C_{16}H_{18}NaO_5$: 313.1046, found: 313.1052.

1.4 Films preparation protocol

The thick films were prepared using the following procedure (Scheme 6):

1. The bioactive monomer (either **1** or **2**) was dispersed in the reactive diluent (PETA) for 10 min in an *ultrasonic* bath, set at 30°C.
2. ACTNR oligomers were added mixing them with a spatula, then the viscous solution was introduced for 15 min in the *ultrasonic* bath.
3. Darocur photoinitiator was injected in the previous mixture, leaving it for other 5 min in the *ultrasonic* bath.

The viscous medium was degassed under light vacuum, and homogeneity of the dispersion was observed by optical microscope. On average 50 mg of pre-polymerization mixture were deposited on a Teflon mold (diameter 1 cm, thickness 0.5 mm) and irradiated by the UV lamp for the required amount of time. The yellowish elastic films were easily removed from the mold with tweezers to perform FTIR spectra and check the complete polymerization.

1.5 Leaching tests protocol

Before evaluating the antifouling properties, the thick films containing 10% of monomer **2** were immerged in de-ionized water at 25°C for 24h. Each film was introduced separately into a 5 mL glass flask containing 1 mL of de-ionized water (18MΩ m^{-1}, Veolia water STI). These flasks were placed in an orbital shaker operated at 50 rpm. The supernatants were separated and analyzed by High Performance Liquid Chromatography (HPLC) to detect the percentage of Darocur 1173 photoinitiator (Scheme 6) and monomer **2** released.

A calibration range of Darocur 1173 was prepared in de-ionized water from 0.86 mg L^{-1} to 17.23 mg L^{-1}. The calibration curve was linear with optical density ranging from 0.0 to 0.85. The solutions in which the disks were immerged were taken and diluted before analysis to be within this range of absorbance[51]. Benzaldehyde and benzoic acid, which have been reported to be the major products from Darocur 1173 photolysis[52] absorb at the same wavelength as Darocur 1173 when analyzed by UV spectrophotometry. HPLC was therefore used to separate Darocur 1173 from its photo-products, in order to quantify it specifically. Benzaldehyde and Darocur 1173 were analysed by injecting 20 µL samples into a ThermoFisher Scientific series instrument equipped with a C_{18} column operated at 30°C (Alltima, 3 µm, 2.1 x 150 mm) and a UV detector (Waters 996) set at 247 nm. The mobile phase was a water/acetonitrile (w/ac) solution with 0.1% TFA, pumped at a flow rate of 0.2 mL/min, whose composition varied as follows: 85:15 w:ac (v/v) to 60:40 w:ac (v/v) for the first 12 min, followed by 5 min of stabilization then 100 ac for 3 min, followed by 5 min of stabilization. Retention times were 16.1 min for benzaldehyde and 16.7 min for Darocur 1173. Calibration was performed between 0.86 and 17.23 mg.L^{-1} with Darocur 1173 and from 1.66 to 16.64 mg.$L^{-1}$for benzaldehyde. Benzoic acid was analyzed in the same manner, setting UV detector at 230 nm. Retention time was 13.4 min. Calibration was done between 1.13 and 22.6 mg L^{-1}.

The monomer **2** released was monitored by HPLC as previously described and a UV detector set a 307.6 nm. Retention time was 24.8 min. The calibration quantified by peak area was linear between 0.213 $mg.L^{-1}$ to 27.214 $mg.L^{-1}$ in acetonitrile.

1.6 Biological assays

Five strains of pathogenic bacteria which pose threat to the human health and are ranked in the drug-resistant list[53] were selected and studied in static conditions in contact with the films: *Pseudomonas aeruginosa* (CIP: A22, PA, Gram negative), *Staphylococcus aureus* (CIP 52.16, SA, Gram positive), *Staphylococcus epidermidis* (CIP: 176.117, SE, Gram positive), *Bacillus subtilis* (CIP, 67.7, Gram positive), *Escherichia coli* (E. coli, CIP, 54.8, Gram negative) from the Luis Pasteur Institute collection. Enzymatic catalase test was performed to check Gram positive strains integrity and oxidase test for Gram negative ones, then three suspensions were prepared in culture media. The following concentrations were determined by comparing the suspension absorbance (at 600 nm for PA et SE, et 650 nm for SA) with the reference one from the literature: PA, $5.2 \cdot 10^6$ UFC/mL; SA, $9.75 \cdot 10^6$ UFC/mL; SE, $7.5 \cdot 10^6$ UFC/mL, respectively. Antibiograms were performed to determine the minimum inhibitory concentration (MIC) of the molecules that were used to make the films. For each compound, 10 µL were deposited in 6 mm diameter holes for pathogenic bacteria and 4 mm for marine ones, made on the nutrient agar (BIOKAR diagnostics-solabia, Allonnes, France) contained in Petri dishes, on which the bacterial suspensions were spread[34]. The two monomers **1** and **2** were dissolved in DMSO in a range of concentration from 2.5 to 40.0 mg/mL; Darocur 1173, PETA, and acrylate oligomers were deposited as pure samples. The inhibition halo diameter was measured after incubation at 37°C for 24h. A strain per Petri dish was used.

Attachment assays were performed using 4 films (dimensions of each film: diameter 1 cm, thickness 0.5 mm) per bacterial strain; 3 films were used to enumerate viable bacteria and one treated to take SEM images (Scanning Electron Microscopy). The bacterial suspension itself was used as growth control (after 3h of incubation at 37°C, without films) and pure ethanol was used as biocide one. 250 µL of bacterial suspension were deposited on the surface of each disk to completely cover it, and the disks were incubated in an oven at 37°C, for 3h. Successively, the 250 µL of bacterial suspension were removed, the disks were transferred in tubes containing 1 mL of nutrient broth and vortexed (Phoenix instrument RS-VF10) at the maximum speed for 30 seconds. The bacterial suspensions taken from the tubes (50 µl) were injected in an automatic spiral plate (easySpiral, Interscience, Saint Nom, France); the appropriate dilutions of cultures were made and spirally plated on nutrient agar plates. The plates were incubated at 37°C, for 24h and the colonies were enumerated using the *easyspiralpro* program.

Marine bacteria used in this work belonged to the LIENSs laboratory collection (University of La Rochelle, France). *Flavobacterium* II2003, and *Bacillus* IV3004 strains were collected from an intertidal temperate mudflat biofilm of the French Atlantic coast. *Alteromonas* IVA014 was isolated from the biofilm associated with the corrosion products formed on carbon steel structures immersed in a French Atlantic harbor. These

marine strains were identified by 16S rRNA gene sequencing. They were grown in Marine broth at 22°C and maintained on Marine Agar (Conda). Bacteria were stored at -80°C and reactivated in a Muller Hunton broth; a relation was established between optical density and number of colonies per mL and three suspensions were prepared. The disks were immerged in 1 mL of Muller Hunton broth and 100 µL of bacterial suspension were added; they remained 3h at 37°C then 1 µL of the supernatant was taken and diluted for the injection in the spiral plate. Four replicates were run each time, plus one not containing the disks (growth control) and a biocide control (1 mL of Muller Hunton broth and 100 µL of ethanol). The plates were left at 37°C and bacteria were counted after 6, 9, 24, and 48h.

The procedure to fix bacteria on the surfaces for SEM images was the following[54]: after incubation and drying, the disks were washed twice with 1 mL of sodium cacodylate buffer (pH 7.4) and immersed for 30 minutes in a 2.5% glutaraldehyde solution in 0.05 M sodium cacodylate buffer (pH 7.4) at RT. The disks were washed again twice with sodium cacodylate buffer, immerged in a series of ethanol/water solutions (30/70, 50/50, 70/30, 90/10, 100) for 15 min in each, and then immerged in hexamethyldisilazane for 30s. The films were coated with gold before observation.

2 Results and discussions

The aim of this work was to covalently integrate a bioactive monomer into a modified natural rubber matrix in order to generate ecofriendly antibacterial/fouling release materials. The used strategy was based on the photopolymerization of a mixture of oligoisoprenes (prepared from NR) and monomers bearing a bioactive function. Acrylate groups were introduced in the structures of the macromonomers and monomers to perform the polymerization. This approach appeared as an attractive alternative because these solvent-free mixtures can be cured within seconds at ambient temperature to yield highly resistant cross-linked polymers. The synthesis of the macromonomers (ACTNR) prepared from natural rubber was already described [34] and will not be presented. The $\overline{M}_n$ of the starting oligomers ACTNR in the present study was 6000 g/mol because it was the minimum molar mass able to give flexible films. In the following sections, firstly the choice of the target monomer including advantages and drawbacks will be discussed. Then the synthesis of the monomers and the thick films will be presented as well as their properties. To conclude, the results of the biological assays will be shown.

2.1 Design and synthesis of monomers derivated from Zosteric acid

As mentioned previously, the investigation of ZA toxicity and its analogs including structure activity relationships studies confirmed the potential of this family of compounds as bacterial growth inhibitors, making them interesting scaffolds for the development of new antibiofouling agents.

The target monomers had to satisfy two criteria: the first one was to provide a ZA-scaffold, maintaining specifically the double bond (C=C) with *E*-configuration, conjugated with the aromatic ring. The second one was that the monomer had to bear an acrylate polymerizable group to assure a covalent link to the matrix. The sulfate group was not introduced as it was mentioned in the literature that it was not necessary for the

biological activity[42]. One of the key-points for the targeted monomers was the choice of the anchor site for the acrylate function: compounds **1** and **2** were designed for this project and their structures are presented in Figure 2.

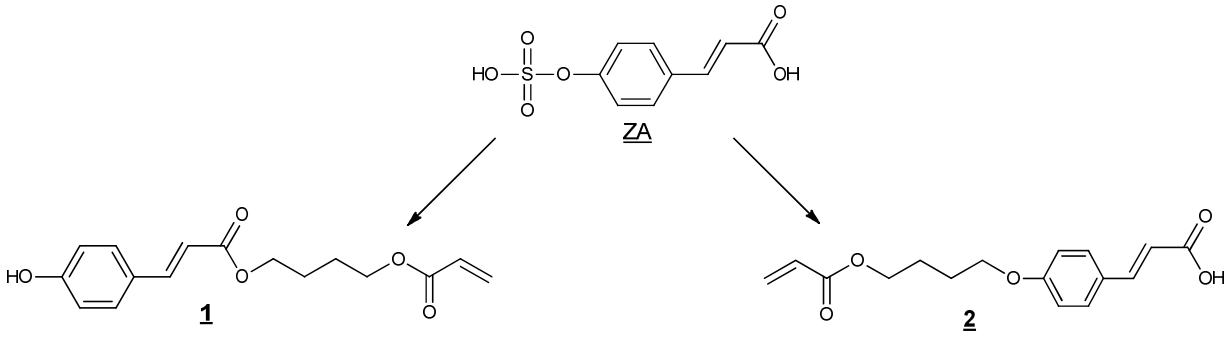

Figure 2: Zosteric acid (ZA) and chemical structure of the two target antibacterial monomers.

For the monomer **1**, the acrylate function was anchored from the carboxylic acid function since it was shown that a *para*-substituted cinnamic acid ester with a hydroxyl group presented some anti-biofilm activities[42]. For the second monomer **2**, the acrylate function was linked from the phenol moiety since it appeared that the presence of the carboxylic acid conjugated to the double bond was important as well for the biological activity[42].

2.1.1 Synthesis of monomer 1

The targeted monomer **1** was prepared according to a strategy in three steps from *para*-coumaric acid (Scheme 1). The synthesis pathway started firstly by the protection of alcohol and carboxylic acid functions with *tert*-butyldimethylsilyl chloride (TBSCl), then the saponification of the silyl ester in basic conditions was performed in order to generate the compound **3**. To introduce the acrylate function, the esterification of **3** with 4-hydroxybutylacrylate in Steglish conditions (DCC/DMAP) was carried out but it failed, whereas in Mitsunobu conditions (DIAD/PPh_3) the product **4** was obtained. The last step consisted in the deprotection of the silylated ether with TBAF, generating the targeted monomer **1** with an overall yield of 75%.

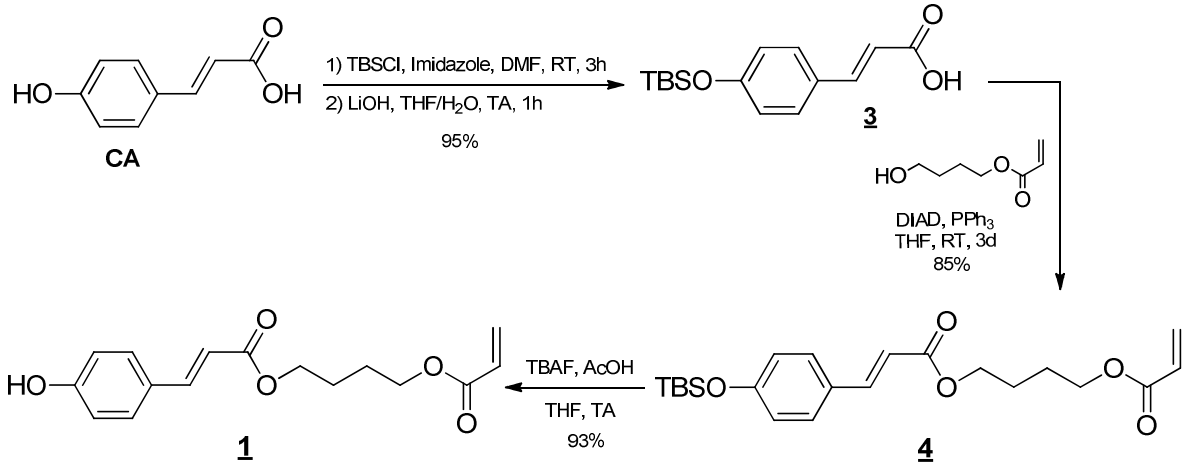

*Scheme 1: Chemical pathway of the synthesis of monomer **1***

2.1.2 *Synthesis of monomer 2*

The monomer **2** could be prepared according to the following retrosynthetic analysis (Scheme 2). The setting up of the carboxylic acid function conjugated to the carbon-carbon double bond for the monomer **2** could be obtained either by malonic synthesis or by a Wittig reaction from the aldehyde function of the molecule **6**. This precursor **6** would be prepared from the commercially available compound **4**.

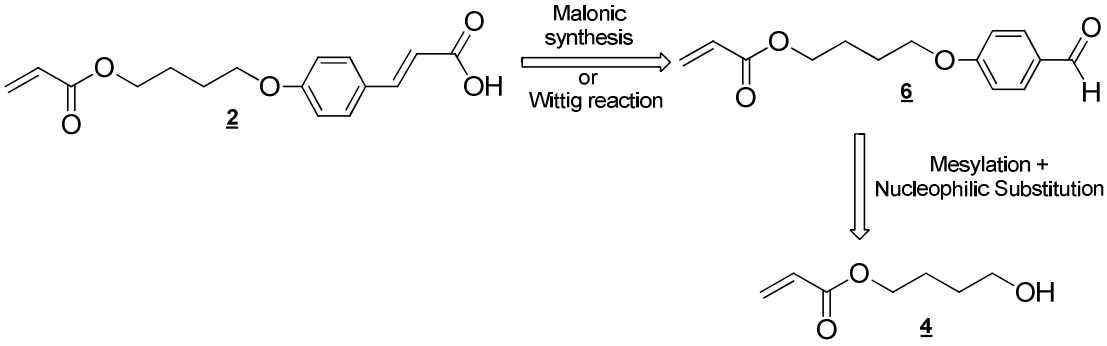

Scheme 2: Retrosynthetic scheme for the synthesis of the monomer 2

For the synthesis of **6** (Scheme 3), the first step was the introduction of a mesylate group from the alcohol function of **4**. Then, the obtained compound **7** was reacted in basic conditions with the 4-hydroxybenzaldehyde. This pathway was the best alternative (93 % overall yield) to obtain **6** since a Mitsunobu coupling (between **4** and the 4-hydroxybenzaldehyde) was also tested and gave **6** with a yield equal to only 47 % after a very long reaction time (7 days).

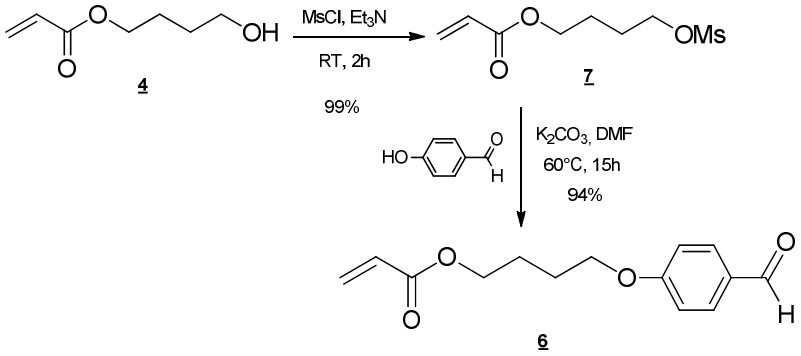

Scheme 3: Preparation of the precursor 6 (monomer 2)

Various reaction conditions for the malonic synthesis were described in the literature using a basic[55, 56] or acidic[57] medium. The different attempts from **6** and malonic acid in basic conditions failed since for each essay the acrylate system was modified (probably by saponification). The use of an acidic medium (AcOH + $MeSO_3H$) allowed us to obtain the monomer **2** but always in mixture with a side-product (Scheme 4). This side-product has been identified and it corresponded to the product **8**, having a methyl group in place of the double bond of the acrylate, due to a transesterification reaction of the monomer **2** with the acetic acid (reaction solvent).

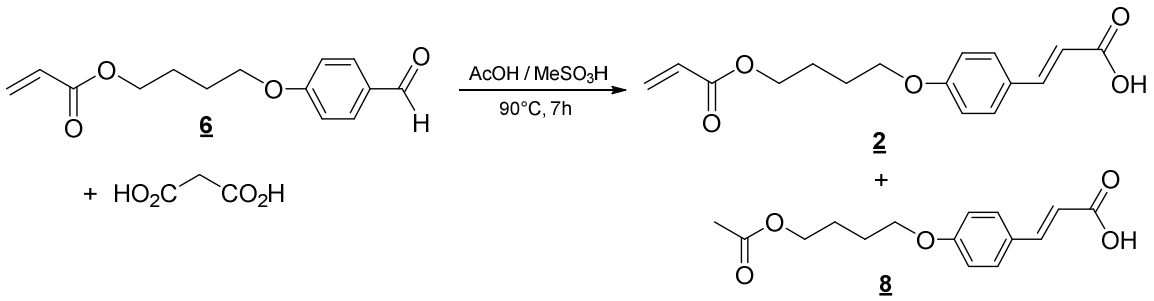

Scheme 4: Malonic synthesis for the preparation of monomer **2**

This approach (malonic synthesis) was unsatisfactory, so another route was considered to synthesize the monomer **2**, the one using a Wittig reaction. The compound **6** was therefore reacted with a phosphonium ylide bearing a *tert*-butyl ester and the product **9** was isolated after purification with a yield of 78% (Scheme 5). The *E* configuration of carbon-carbon double bond was confirmed since a coupling constant (^3J = 16 Hz) was observed between the two alkenic protons on the ^1H NMR spectrum. The last step consisted in the hydrolysis of the *tert*-butyl ester to generate the monomer **2**. Bearing two ester functions, the compound **9** had to be selectively hydrolyzed. The choice of the *tert*-butyl ester as a protecting group for the carboxylic acid was therefore justified since it could be cleaved in acidic medium. Finally, the monomer **2** was successfully isolated with 89% of yield by deprotection of *tert*-butyl ester, using trifluoroacetic acid.

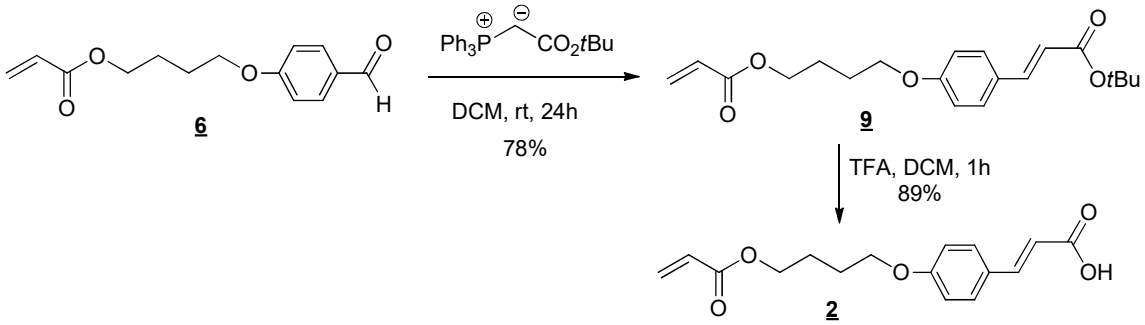

Scheme 5: Wittig reaction and acidic hydrolysis for the synthesis of monomer **2**

2.2 Thick films: formulations and kinetic study of the photopolymerization

In previous works[34, 47-49, 58, 59], it was demonstrated that the films obtained from ACTNR oligomers without adding any biocide groups presented a low but noticeable antibiofouling activity. This activity was significantly enhanced by incorporating a bioactive function on the NR network, such as the quaternary ammonium groups at the oligomers chain ends or a monomer containing a guanidinium group. In the case of the incorporation of the guanidinium monomer to the $ACTNR_{6000}$ network for conferring the antimicrobial activity, it was needed to add PETA as reactive diluent in the formulation to obtain homogenous films[34]. Furthermore, it was observed that 10% weight of guanidinium monomer presented the best value to generate antibacterial activity and maintain interesting mechanical properties of natural rubber. Knowing the data relative to the guanidinium thick films, in the present work, two families of antifouling polymer materials based on natural rubber were envisioned, containing 10% weigh of monomer **1** or **2**, in presence of PETA, to prepare thick films in view of future applications (Scheme 6). PETA was added to better disperse the

monomers **1** or **2** in the pre-polymerization mixture, remaining covalently bound to the network at the same time. Darocur 1173 was chosen as a photoinitiator because its absorption spectrum (located in the UV region) is different compared to the ones of $ACTNR_{6000}$ oligomers and both monomers. Furthermore, among the common photo-initiators, it is a liquid and it can be easily dispersed in the viscous polymerization mixture. The percentage retained for all formulations was 2.5% (weight) because it represented a good compromise between a lower amount (1%) that required longer polymerization times, and a higher amount (5%)[60, 61] that allowed shorter irradiation times but increased the amount of unreacted photoinitiator released in the environment.

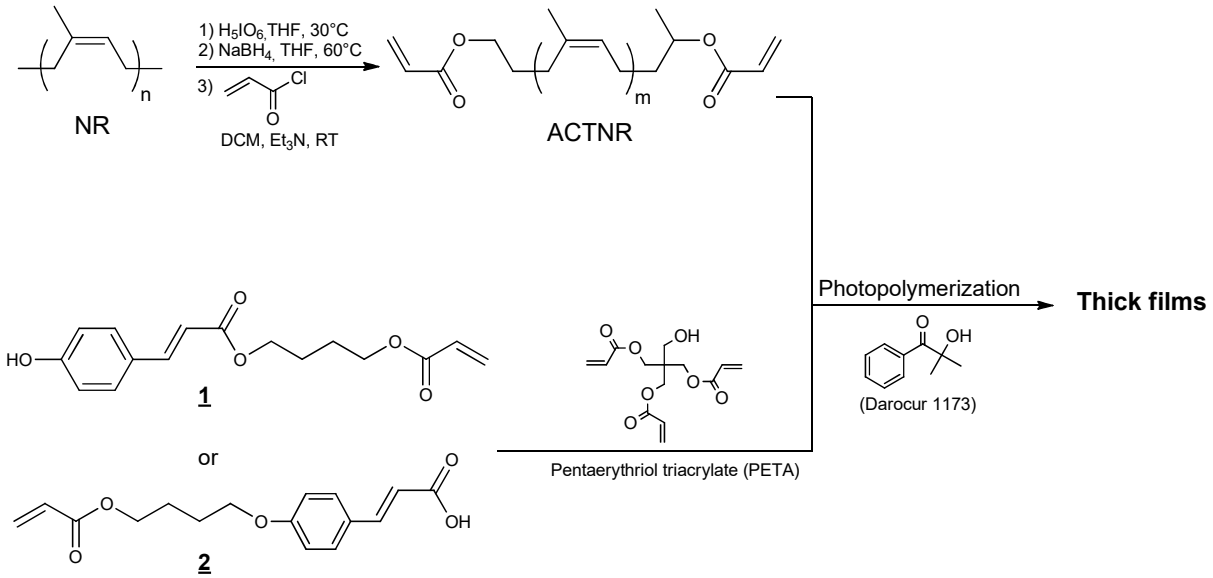

Scheme 6: General procedure for the synthesis of the antifouling coatings.

The kinetic study of the photo-polymerization, monitored by FTIR-ATR, was carried out using the formulations described in Table 1, in order to verify the conversion of acrylate groups in relation to the polymerization time. During the polymerization reaction, the purpose was to polymerize only the acrylate group without touching the carbon-carbon double bond in the polyisoprene repeating units to maintain the NR mechanical properties.

*Table 1: General composition of films containing the monomer **1** or **2** (% = weight percentage)*

Composition	F_{10} Monomer **1**	F_{10} Monomer **2**
$ACTNR_{6000}$	67.5 %	67.5 %
Darocur 1173	2.5 %	2.5 %
PETA	20 %	20 %
Monomer 1	10 %	0 %
Monomer 2	0 %	10 %

A comparison of the FTIR spectra of the monomers **1** and **2**, *para*-coumaric acid and $ACTNR_{6000}$ was performed and is presented in Figure 3. These data enabled to make sure that the addition of the monomers **1** or **2** in the ACTNR matrix did not cover the two bands used for the conversion calculation, corresponding to $=C-H_2$ stretching of the acrylate group at 1405 cm^{-1} and to the reference peak located at 1376 cm^{-1} [49,58] whose intensity remains constant during irradiation. It was also confirmed that the main aromatic bands $\delta(CC)_{ar}$ were located at 1601 and 1509 cm^{-1} (Figure 3C). Both monomers **1** and **2** presented the band at 1630cm^{-1}, characteristic of the C=C double bond conjugated with the carboxylic group (Figure 3B). These assignments agreed with the data reported by R. Świsłocka *et al.*[62] concerning the spectroscopic (FT-IR, FT-Raman, ^{1}H and ^{13}C-NMR) and theoretical studies of *p*-coumaric acid and alkali metal *p*-coumarates.

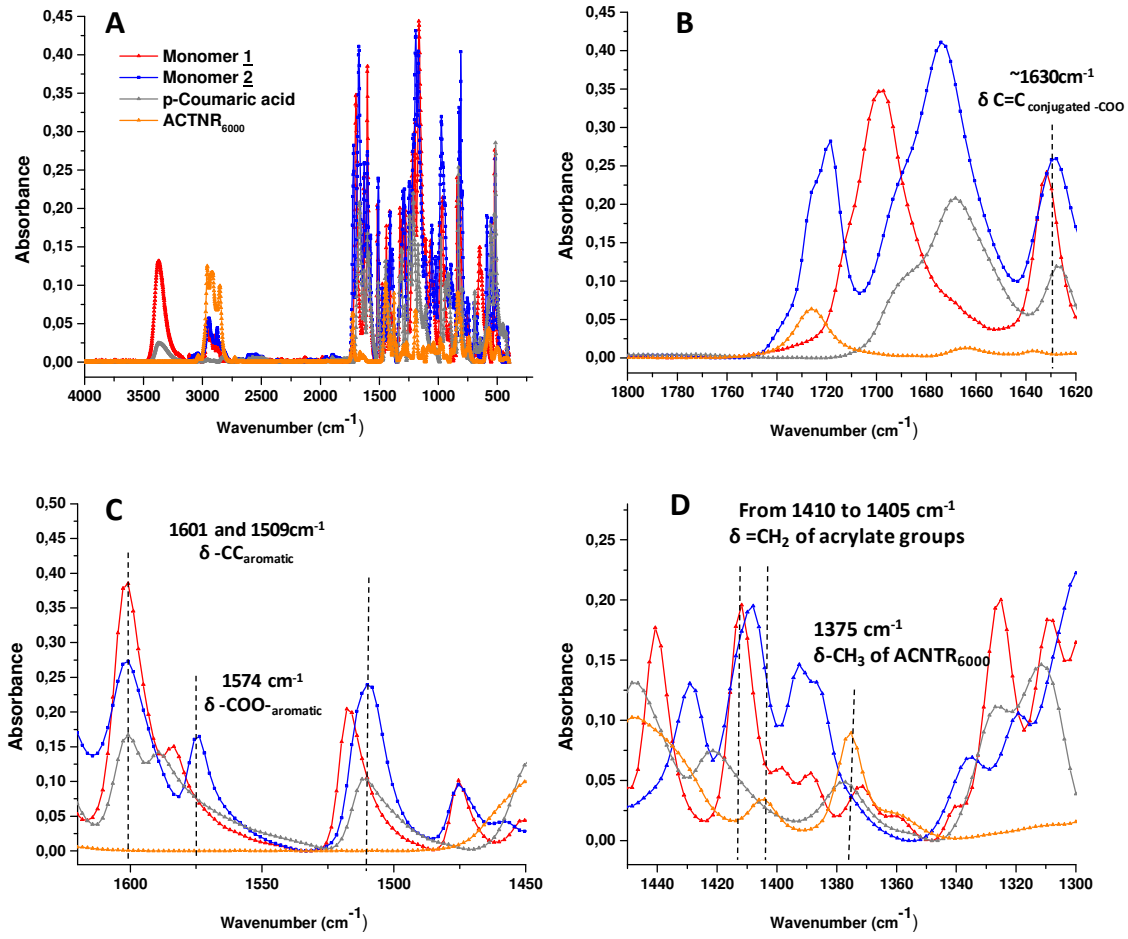

*Figure 3: Comparison of FTIR spectra of monomers **1** and **2**, para-coumaric acid and $ACNTR_{6000}$, (**A**): entire IR spectrum ;(**B**, **C**, **D**): zoom, respectively for 1800 – 1610 cm^{-1} region, 1620-1450 cm^{-1} region and 1450-1300 cm^{-1} region. Light intensity **I=29.4 mW/cm²**.*

Thick films were prepared in Teflon™ molds, using the two formulations **F_{10} Monomer 1** and **F_{10} Monomer 2** with a dimension of 1cm of diameter and 0.5mm of thickness. IR spectra were performed on the face A (surface directly exposed to the UV-lamp) and the face B (surface in contact with the mold). The light intensity was kept constant at 29.4 mW/cm^2. The percentage of conversion of the polymerization mixture was calculated with the equation (**1**) (see details in Experimental section), using the two bands at 1405 cm^{-1} and at 1375 cm^{-1}.

With the formulation **F_{10} Monomer 1**, containing 10% of monomer **1**, it was observed that the photopolymerization reaction was not complete after 25 min, for both faces, confirmed by the presence of the band of the acrylate group at 1405 cm^{-1} (Figure 4). Conversely, the intensity of the characteristic bands of $ACTNR_{6000}$ including the reference band at 1375 cm^{-1}, and in the range of 3010-2775 cm^{-1}, decreased, suggesting a degradation of the polyisoprene motif that was not our objective. This slowing down of the reaction rate could be explained by the presence of the phenol group (**-C_6H_4-OH**) in the structure of the monomer **1**. Phenols are known for their role of polymerization inhibitors[63, 64], in particular, R.A. Bird *et al.*[65] studied the effect of phenols on the polymerization of vinyl acetate. They demonstrated that phenols acted as fairly strong retarders in radical polymerization due to the attack of polymer radicals to phenols group by hydrogen abstraction. In view of these results, the use of monomer **1** was given up and for the rest of the study only the F_{10} Monomer **2** formulation was used.

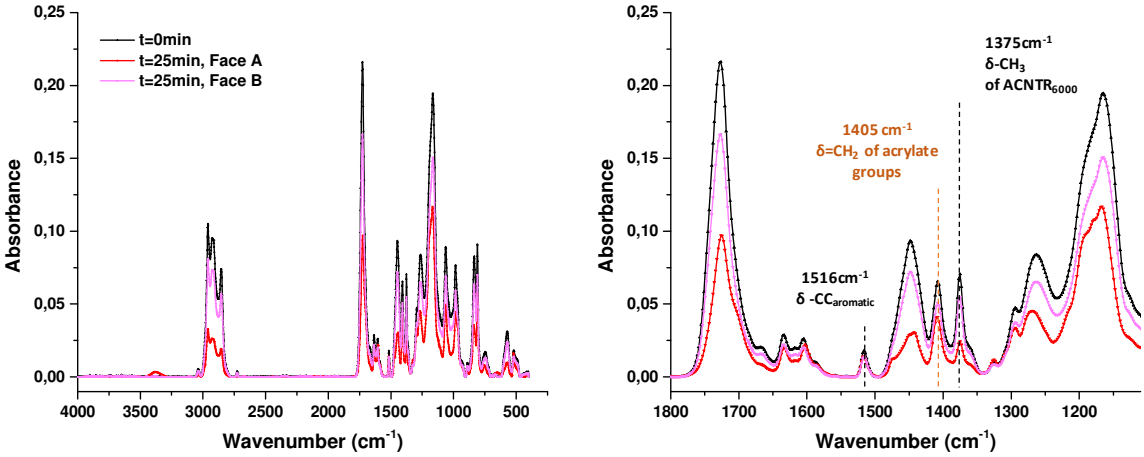

*Figure 4: Changes of the IR absorbance for the acrylate group upon irradiation in **F_{10} Monomer 1** formulation (peak at 1405 cm^{-1}). **Left**: entire IR spectrum; **Right**: zoom of the 1800 – 1200 cm^{-1} region. Light intensity **I=29.4 mW/cm²**. Films dimensions of 1cm diameter and 0.5mm thickness.*

With F_{10} Monomer **2** formulation, it was noticed that the conversion was higher on face A than face B. This difference was due to the direct exposition of the face A to the UV-light whereas the face B was in contact with the Teflon™ molds. Indeed the pre-polymerization mixture was opaque and viscous, so a part of the light was absorbed and the lower face received a less intense radiation (conversion profile upon irradiation, using F_{10} Monomer **2** formulation is reported in Supp. Info). It was clearly shown that after 10 min, roughly 93% conversion of the total number of acrylate double bonds was reached on the face A and around 80% for the face B.

A great number of replicates was needed to test biological properties, so it was decided to prepare the films with another UV-lamp equipped with a sliding belt, having more powerful light intensity of 0.313J/cm^2. However, with this equipment, it was noticed that after 47s upon irradiation, the carbon-carbon double bond of the repeating unit started to disappear (Figure 5). The deformation of spectrum profile in the range of 3100-2800 cm^{-1} was observed. Therefore, the irradiation was stopped before the complete conversion of acrylate groups was reached. For these reasons, the first type of thick films using F_{10} Monomer **2** formulation

was obtained upon 47s irradiation with 96% conversion on the faceA and around 80% for the face B (Type I).

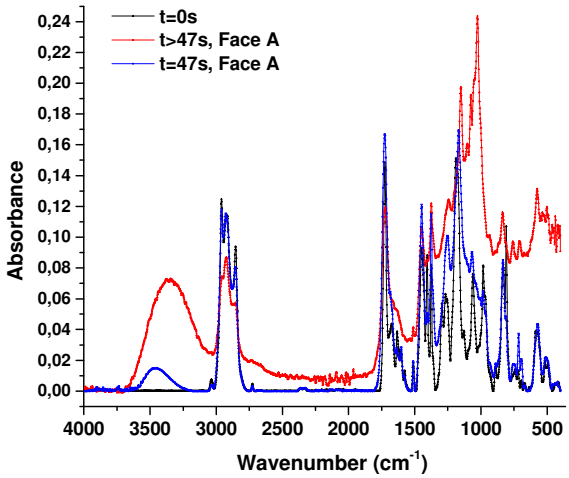

Figure 5: The IR spectrum profile change completely upon irradiation after 47s (Red line), compared with that at 0s (Back line), at 47s (Blue line). It is clearly shown that the degradation of the carbon-carbon double bond of the repeating unit started.

In order to improve the conversion of the face B and study the effect of crosslinking rate of bioactive monomer on leaching and biological tests, a second series of thick films was obtained by submitting again the face B of the Type I to 4 min irradiation, with light intensity of 29.4 mW/cm^2. FTIR analyses showed 96% conversion for face A and around 92% for face B for films Type II, without degradation of the C=C bond of the isoprene unit.

2.3 Leaching test results

The polymer films were synthesized from NR based oligomers and the monomer **2** *via* a photopolymerization in presence of Darocur1173 as photoinitiator. As mentioned in the introduction, the main goal of this work was to develop new fouling release materials non-releasing, ecofriendly and nontoxic, therefore, leaching tests were performed of films immersed in water to detect if any component had been released from our materials. In order to make sure that in the conditions of the biological tests no leaching was occurring from the polymers, and to ensure that the biological activity was due to the active monomer rather than the unreacted photoinitiator released, the films were immersed in water for 24h before being tested. Fourteen supernatant samples were taken to analyze the released percentage of Darocur 1173, its photo-degradation products benzaldehyde and benzoic acid,[52] and the monomer **2**. The results, presented in Figure 6, showed that after 24h of immersion in water, around 70% of Darocur 1173 from films Type I was released and 40% from films Type II. A very small fraction of Darocur gave the photodegradation products, as only around 3.0% of the maximum amount of benzoic acid that could be released from films Type II, and no significant values (< 0.4%) from films Type I, were detected. No release of benzaldehyde was detected. Concerning the release of the monomer **2** (Figure 6 C), around 0.5% was found for films Type I and only

0.2% for the films Type II. These differences can be explained by a greater conversion of acrylate groups during the photopolymerization process on the films Type II and so a lower release of the film components.

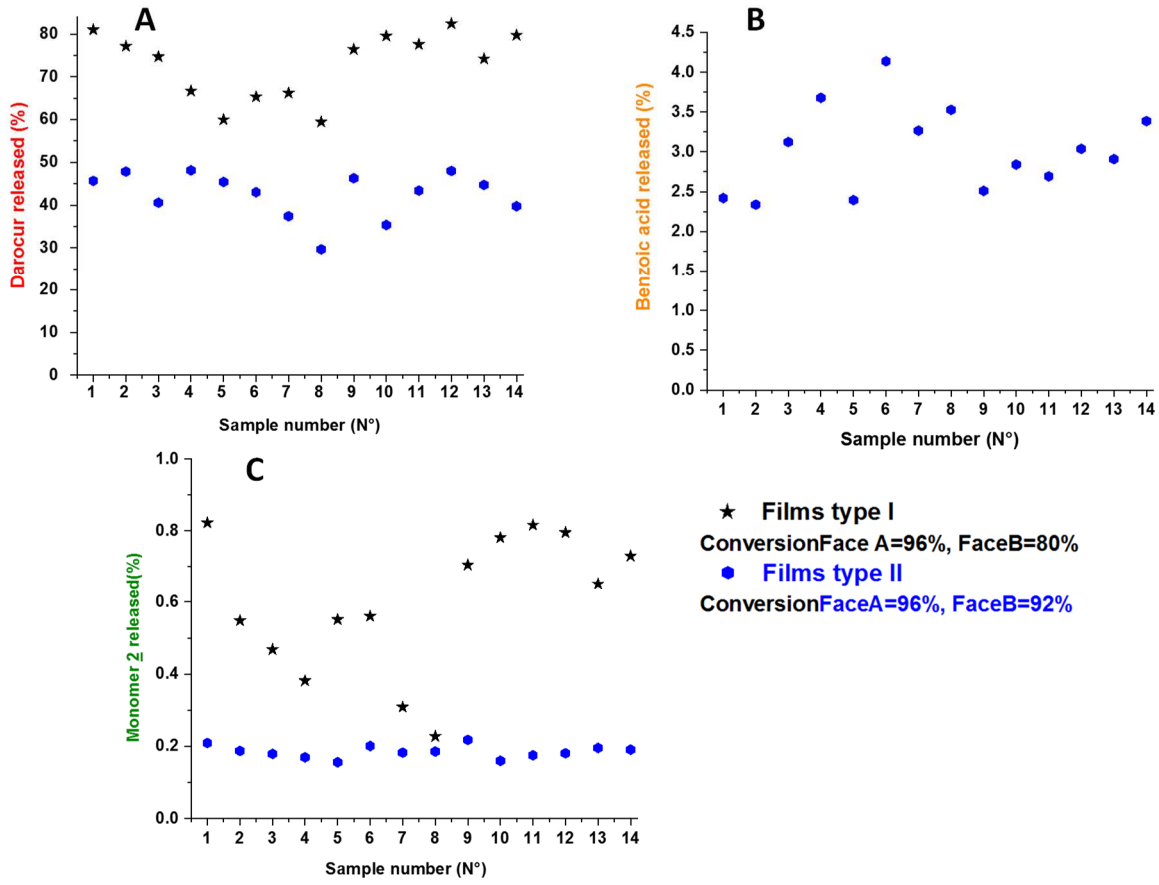

*Figure 6: Time course of Darocur 1173 (**A**) and benzoic acid (**B**) and Monomer **2** (**C**) leaching into de-ionized water after 24h from thick films (0.5mm thickness x1.0mm diameter) using F_{10} Monomer **2** at 25°C, detected by HPLC. Benzoic acid released for films type I <=0,4% (few of samples out of calibration curve).*

2.4 Coatings thermal properties and surface contact angle

In order to determine the thermal stability (degradation temperature) of the films and thus studying the effect of adding the monomer **2** on $ACNTR_{6000}$ matrix, TGA analyses were performed on three categories of films: films type I, type II and reference films that contained 77.5% of ACTNR6000, 2.5% of Darocur and 20% of PETA without monomer **2** (Films Ref).

The TGA curves are presented in Figure 7. They were obtained at a heating rate of 10° C min^{-1}, from 40°C to 800°C, under nitrogen atmosphere. No difference between the films of Type I and Type II was observed. The 10% weight loss values for all the samples were summarized in the Table 2. It indicated that the addition of monomer **2** reduced insignificantly the thermal stability of polyisoprene film (346 versus 348°C). The thermograms (Figure 7) showed that all films remained stable up to 200 °C. Two degradation steps located at

250°C and at 374°C were present for both films containing 10% of monomer **2**, in comparison to only one step for the film Ref. The weight losses for the first and second step were 3.3% and 72.0% w/w, respectively.

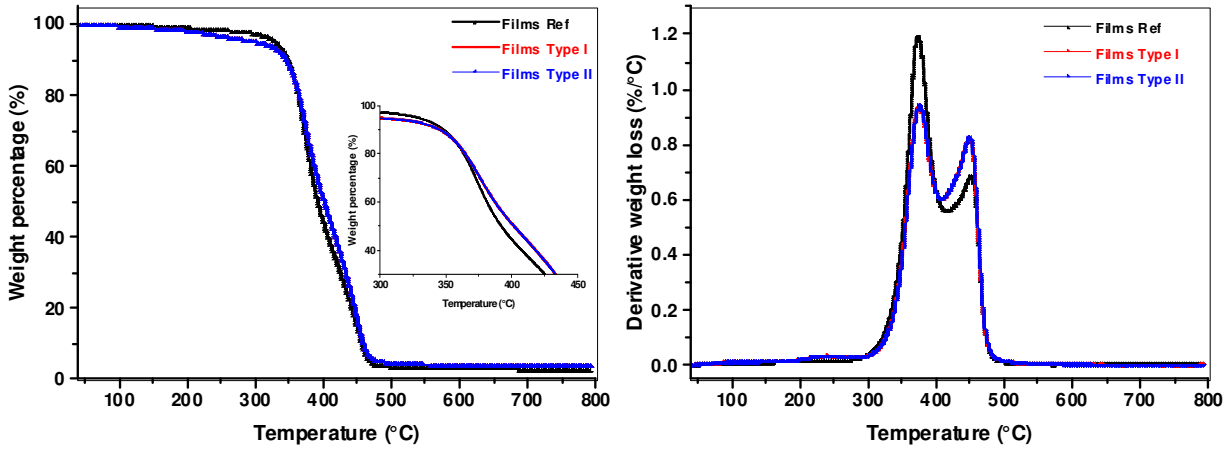

*Figure 7: Thermograms of two types of films containing 10% of monomer **2**, compared to films without it (Films Ref).*

Sathish *et al.*[66] demonstrated that when the decomposition of *p*-coumaric acid took place, for the first step, at 181°C there was a 56.89% mass fraction loss, which was attributed to the decomposition of -OH phenolic group. In the second stage the decomposition started at 181°C and ended at 266°C, corresponding to the breakage of the carboxylic group from the phenyl ring. Furthermore, Ouimet *et al.*[67] pointed out that by chemically incorporating *p*-coumaric acid into the backbone of a poly(anhydride-ester), the obtained polymer exhibited a decomposition temperature of 302 °C and a T_g equal to 57 °C for a 26.7 kDa mass. The first decomposition step observed at 250°C in our case concerned probably the degradation of the monomer **2** moiety and the other steps corresponded to the polyisoprene degradation. The Table 2 summarizes the degradation temperatures and corresponding weight loss of each type of films, compared to the film reference.

Table 2: TGA and contact angle data of different films.

Sample	Decomposition temperature (°C)					
	At the weight loss				T_{max}[b] (°C)	Contact angle
	T_5[a]	T_{10}[a]	T_{50}[a]	T_{90}[a]		(°)
Films Ref	329	348	392	457	374	79
Films Type I and II	309	346	400	460	374	53

T_x[a]: Decomposition temperature at the x% weight loss: a) data obtained from TGA curve, b) data obtained from DTG curve.

The wettability of the three types of films used for TGA analysis was also determined by measurement of the contact angle (see figure in section 3 of Supp. Info). The obtained data are presented in Table 2. As for TGA results, no difference of wettability for films Type I and Type II was observed. For all samples, a value of contact angle less than 80° was found, that often denoted a rather hydrophobic character. However, a significant decrease of contact angle was observed by adding 10% of monomer **2** in the polymer matrix (53° versus 79°), indicating a higher level of hydrophilicity. This difference could be explained by the presence of the carboxylic group (-COOH) of the monomer **2** at the films surface, as well as in bulk.

2.5 Biological activity

2.5.1 Pathogenic bacteria

The films containing the monomers with the Zosteric acid scaffold were analyzed in order to evaluate their biological activity. Five strains of pathogenic bacteria which pose threat to the human health and are ranked in the drug-resistant list[53] were selected and studied in static conditions in contact with the films: *Pseudomonas aeruginosa* (CIP: A22, PA, Gram negative), *Staphylococcus aureus* (CIP 52.16, SA, Gram positive), *Staphylococcus epidermidis* (CIP: 176.117, SE, Gram positive), *Bacillus subtilis* (CIP, 67.7, Gram positive), *Escherichia coli* (E. coli, CIP, 54.8, Gram negative).

Antiobiograms were performed to see the action of each component of the formulation alone, in case it was accidentally released from the films, and to observe the action of each monomer alone before its integration in the $ACNTR_{6000}$ matrix, also to confirm that it had an activity of its own, which was maintained once inserted in the polymeric matrix. The results of the antibiograms (table 6.3 SI) confirmed the toxicity of pure Darocur 1173 (BASF Safety data sheet[68]), which inhibited all the three bacteria. However, considering the amount of unreacted Darocur released by the coatings in the assays conditions, and the washing step to which they were submitted before testing, the Darocur activity does not influence the results, as already discussed in depth in our previous work[34]. The pure crosslinker PETA was active against SA and SE, while the acrylate oligomers inhibited only SE and had no effect on the two others. Trifluoroacetic acid was used as growth inhibition control and showed in all cases the largest inhibition halo.

The monomers **1** and **2** being solid powders were dissolved in DMSO to be deposited in the wells of the agar plates, in a range of concentrations from 2.5 mg/mL to 40.0 mg/mL. The results of the antibiograms are presented in Figure 8 (inhibition halo radius observed in relation to the monomer concentration), in Figure 6.1SI, and in tables 6.1SI and 6.2SI. The solvent DMSO alone did not cause any inhibition halo so it was ensured that its presence did not affect the microorganisms. Monomer **1** exhibited a higher activity than monomer **2** against most of the five bacterial strains in all concentrations, especially against Gram positive ones. *S. aureus* was particularly sensitive towards monomer **2** even at 2.5 mg/mL.

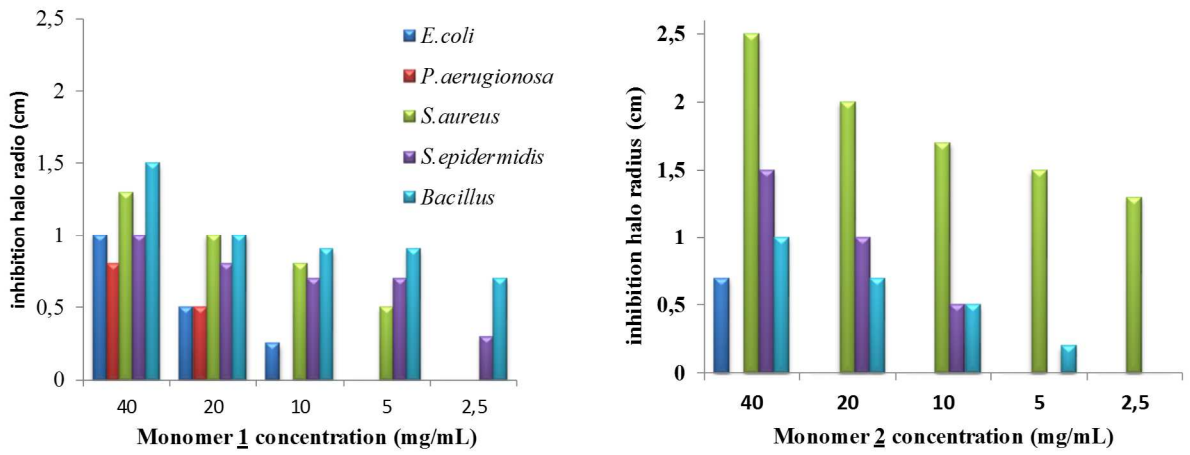

*Figure 8: Antibiograms of monomers **1** (Left) and **2** (Right) for five strains of pathogenic bacteria. No inhibition halo of DMSO solvent was observed (d = 0 cm).*

Despite the inferior activity showed by the monomer **2**, only thick films containing 10% of this monomer were prepared and tested due to the difficulty in obtaining a complete polymerization with the monomer **1**.

A procedure was established to incubate the films with the bacterial suspensions and to calculate the number of surviving cells that remained attached to the surfaces after incubation for 3h at 37°C (Figure 9). Being aware of the results of the leaching tests, it was decided to submit the disks to a washing step (one day immerged in de-ionized water under gentle stirring) before performing the assays, in order to eliminate all the unreacted Darocur photoinitiator and to be sure that the observed activity was not an artefact.

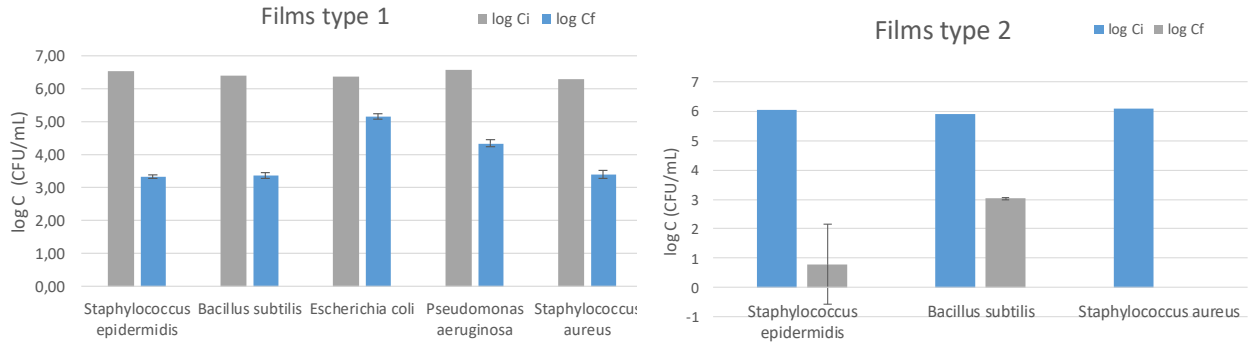

*Figure 9: Antibacterial activity of the two types of films prepared with **F_{10} monomer 2** formulation. Ci is the initial concentration of bacteria and Cf is the final concentration after contact with the films. Errors bars represent standard deviation.*

The bacterial suspension itself was used as growth control, and considering the appropriate dilutions, the number of colonies developed from the bacteria collected at the surface of the disks after the assays was compared to the number of the control. A considerable diminution of the suspension concentration was observed for all bacteria. The most affected strains were *S. epidermidis, S. aureus* and *Bacillus subtilis.* These results confirmed the trend of bacterial attachment on ACTNR matrices that was found in previous studies performed either on the simplest formulation in disks containing only $ACTNR_{6000}$ without any bioactive molecule[48] or in disks prepared adding 10% of guanidine antimicrobial monomer[34]. Moreover, these new coatings exhibited also a great antibacterial activity against *Bacillus subtilis*. It was reported in the

literature that the *para*-coumaric acid showed MIC (Minimum Inhibitory Concentration) value of 20 µg/mL[69, 70], against *Bacillus subtilis.* Hence, this effect can be attributed to the presence of monomer **2** at the surfaces and not only in the bulk of the material.

Based on the first results obtained, the films Type II containing also 10% of monomer **2** were tested with only three of the most effective pathogenic bacteria, *S. epidermidis, S. aureus* and *Bacillus subtilis*. The films Type II showed an excellent antibacterial property, higher than films Type I as expected. No *S. aureus* was found on the surfaces after contact with films and only 0.01% of the bacteria of the initial suspension of *S. epidermidis* and *Bacillus subtilis* remained attached. As previously demonstrated, after 24h, only 0.2% of the maximum amount of the monomer **2** was released (~0.01mg), so during the biological tests this release could not affect the antibacterial activity.

Observation of the surfaces of selected disks after immersion in the bacterial suspensions was regularly made by scanning electron microscopy, in order to have complementary information to assess the antibacterial activity. The same treatment for the biological tests was applied to all the replicates and some of them were observed after applying the procedure to dry the bacteria and fix them in order to obtain the images. Numerous bacteria were found on disks not containing the zosteric acid monomer (data not shown), whereas the visual observation supported the quantitative data from the attachment assays on the disks containing the monomer **2**: after carefully looking at the entire surface, no bacteria were found (Figure 10 A-E for magnification x500 and Figure 5.1 in Supp. Info for bigger magnification), except for PA, for which few were observed (Figure 5.1 C in Supp. Info). In addition, these images allowed monitoring the morphology of the surfaces after immersion, and no significant change was noticed after contact with water or decontamination treatments (repeated washings with ethanol). As the films were obtained by spreading the pre-polymerization mixture with a spatula, the presented morphologies showed a not perfectly smooth surface as expected, with features size and shape not influencing the bacterial attachment.

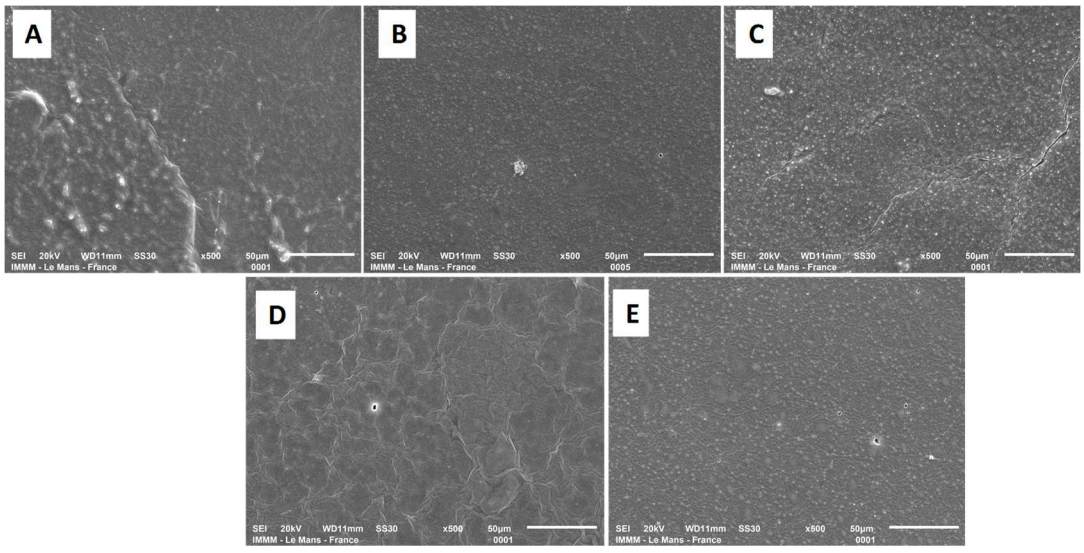

*Figure 10: Micrographs of disks Type I containing 10% of monomer **2** after incubation with: a) Bacillus b) E. coli c) PA, d) SA, e) SE. Zoom at 50µm with 500 x. No bacteria are visible.*

Further studies will be carried out in the follow up of this preliminary work to assess if the attached bacteria are dead or alive, if their growth is influenced, and to understand the mechanism of action of the surfaces.

2.5.2 *Marine bacteria*

One of the objectives of this research work was to obtain one material for two different applications. Pathogenic and marine bacteria were tested to verify respectively the antibacterial property and the activity against marine fouling (for which the first step is bacterial colonization[71]). At this stage, only *in vitro* tests with selected bacteria used in our previous work were performed, in static conditions. In the follow up of this research work, other microorganisms such as microalgae and marine fungi will be used and *in vivo* assays will be carried out.

The antibiograms were performed for the marine bacteria using the two monomers and also in this case it was found that the monomer **1** was more effective than monomer **2**, as an inhibition halo was observed starting from the concentration of 5 mg/mL (Figure 11). *Bacillus* was the most affected by both monomers and a similar effect was exerted by *Flavobacterium* and *Alteromonas*.

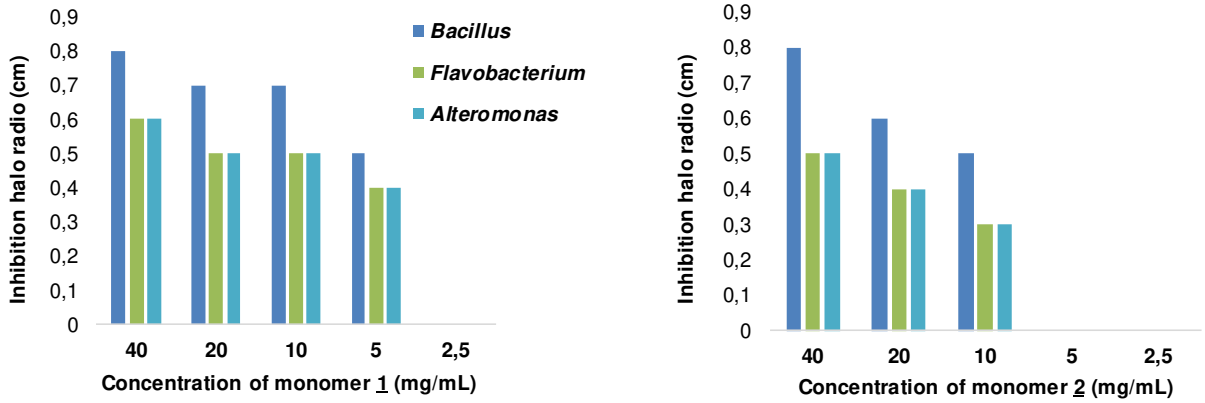

*Figure 11: Antibiograms of monomer **1** (Left) and monomer **2** (Right) of three strains of marine bacteria: Bacillus, Flavobacterium, Alteromonas in the range of concentration from 2.5 to 40 mg/mL in DMSO.*

Having shown that the chosen structures had an antibacterial action, films containing 10% of monomer **2** were tested in order to see if the effect was maintained. The films were incubated for 3h at 37°C with the bacterial suspensions, then the bacteria attached to the surface were counted and their growth was monitored for 2 days (Figure 12). It was found that the growths of *Alteromonas* and *Flavobacter* were visibly affected by the presence of the disks in comparison to the growth control, whereas *Bacillus* was not influenced. The statistical analyses relative to the data presented in Figure. 12 are reported in Supp. Info, section 7.

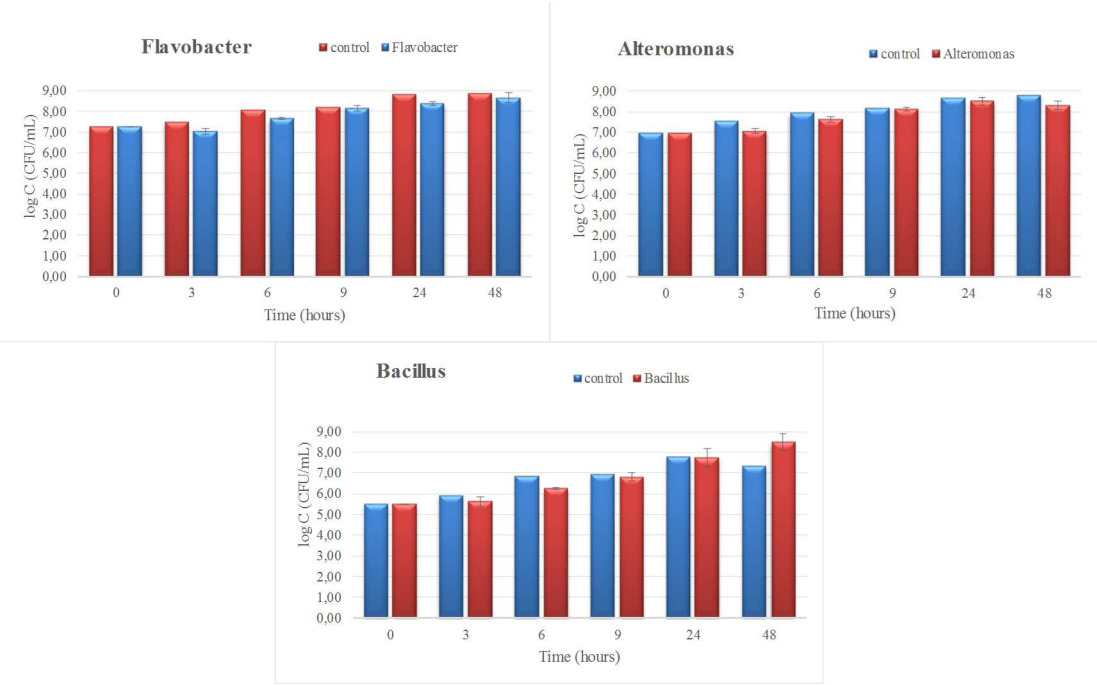

*Figure 12: Growth of the marine bacteria after contact with films containing 10% of monomer **2** or control not containing it. The error bars represent the standard deviation.*

These results were confirmed again by microscope observation but when SEM images of selected disks were taken (Figure 5.2 in Supp. Info), it was realized that a solid deposit of culture medium was present on some of the surfaces. It was later discovered that the formulation used for its preparation caused this problem that affected the quality of the images. No *Alteromonas* nor *Bacillus* were observed while *Flavobacter* formed a biofilm but only near the culture medium deposit. This may mean that there is an anti-adherence effect and the presence of *Flavobacter* is connected to the localized concentrated amount of "nutrients" for the microorganisms, as it is not present elsewhere on the surface. Further experiments are currently being carried out in order to explain these encouraging preliminary results, also increasing the amount of monomer **2** in the formulation up to the optimum compromise between increased biological activity and good elasticity and mechanical properties.

3 Conclusions

In order to prepare new bio-based materials displaying antibacterial / fouling release properties, two bioactive monomers were designed and synthesized from Zosteric acid scaffold (an antifouling agent). These two new tailor-made monomers **1** and **2** were successfully and respectively obtained with a 75% overall yield in three steps from *para*-coumaric acid and a 65% overall yield in four steps from 4-hydroxyl benzaldehyde. Both monomers were used in photopolymerization reactions with macromonomers coming from natural rubber and Darocur 1173 was used as photoinitiator. The polymerization kinetics were followed by FTIR to calculate the percentage of conversion of the total number of acrylate double bonds. The conversion was not complete for the monomer **1** whereas the monomer **2** was successfully incorporated in the natural rubber matrix. Biological, thermal and wettability tests were performed with thick films

containing 10% of monomer **2**. These films displayed excellent antibacterial and antifouling activities against three strains of pathogenic bacteria: *S. aureus (SA), S.epidermidis*, *Bacillus subtilis*. No SA bacteria were found on the surfaces after contact with films and only 0.01% of the initially bound bacteria from the *S.epidermidis* suspension and from the *Bacillus subtilis* suspension remained attached to the disks. Three marine bacteria were also tested; *Bacillus* was the most affected by both monomers and a similar effect was exerted by *Flavobacterium* and *Alteromonas*. Growth curves were traced after contact of the bacteria with the surfaces and it was found that the growths of *Alteromonas* and *Flavobacter* were affected by the presence of the disks in comparison to the growth control, whereas *Bacillus* was not influenced. To confirm that this antibacterial activity was due to the active monomer rather than the photoinitiator released, the films were immersed in water for 24h before testing. Fourteen supernatant samples were taken to analyze the released percentage of Darocur 1173, its photo-degradation products benzaldehyde and benzoic acid and the monomer **2**. After 24h of immersion in water, around 40% of Darocur 1173 from thick films was released. Benzoic acid was less than 0.4% of the total amount of benzoic acid and no release of benzaldehyde was detected. Nevertheless, a minor amount of the monomer **2** was observed after 24h (around 0.2%) confirming that monomer **2** was covalently bound to the natural rubber matrix. These films remained stable up to 200°C and decomposed completely at 374°C. A significant decrease of contact angle was observed by adding 10% of monomer **2** in the polymer matrix (53°versus 79°), indicating a higher level of hydrophilicity due to the presence of the carboxylic group (**-COOH**) of the monomer **2** at the films surface, as well as in bulk. The strategy presented herein was based on the co-polymerization of bioactive monomers with the isoprenic macromonomers from natural rubber. In this way, the biological activity was present in the bulk as well as on the surface of the material. Bio-sourced antibacterial and antifouling elastomers, with non leaching bioactive groups (since covalently bound to the matrix) are promising materials and coatings for many industrial applications.

Acknowledgements

The authors wish to thanks Bruno Gace and Emilie Choppe for their help during some syntheses, Lionel Guilmeau for the realization of the Teflon™ molds and Clement Brière for the help with the equipment in the laboratory. Many thanks to Alexandre Benard and Mireille Barthe for SEC analyses, Sullivan Bricaud for NMR spectra (IMMM, NMR platform), Patricia Gangnery for mass spectra (IMMM, Mass spectrometry platform), Anthony Rousseau for taking SEM images (IMMM, Electronic microscopy platform). The authors are grateful to Dr. Alexis Colin of the Center of Transfer of Technology of Le Mans (CTTM) for the use of the UV curing equipment. Lucie Olivier is especially thanked for performing the biological tests and the Lycée Notre Dame (Le Mans) for the possibility to use their laboratory and equipment. The image of the alga Zostera marina has been taken by Dr. Eduardo Infantes Oanes of the Department of Marine Sciences of the University of Gothenburg, Kristineberg Station, Sweden, and the authors acknowledge him for the permission to use it in the graphical abstract.

References

1. Almeida, J. R.; Correia-da-Silva, M.; Sousa, E.; Antunes, J.; Pinto, M.; Vasconcelos, V.; Cunha, I., Antifouling potential of Nature-inspired sulfated compounds. *Scientific Reports* **2017,** *7*, 42424.

2. Vilas-Boas, C.; Sousa, E.; Pinto, M.; Correia-da-Silva, M., An antifouling model from the sea: a review of 25 years of zosteric acid studies. *Biofouling* **2017,** *33* (10), 927-942.

3. Nurioglu, A. G.; Esteves, A. C. C.; de With, G., Non-toxic, non-biocide-release antifouling coatings based on molecular structure design for marine applications. *Journal of Materials Chemistry B* **2015,** *3* (32), 6547-6570.

4. Magin, C. M.; Cooper, S. P.; Brennan, A. B., Non-toxic antifouling strategies. *Materials Today* **2010,** *13* (4), 36-44.

5. Qian, P.-Y.; Chen, L.; Xu, Y., Mini-review: Molecular mechanisms of antifouling compounds. *Biofouling* **2013,** *29* (4), 381-400.

6. Cole, N.; Hume, E. B. H.; Vijay, A. K.; Sankaridurg, P.; Kumar, N.; Willcox, M. D. P., In Vivo Performance of Melimine as an Antimicrobial Coating for Contact Lenses in Models of CLARE and CLPU. *Investigative Ophthalmology & Visual Science* **2010,** *51* (1), 390-395.

7. Pavithra, D.; Doble, M., Biofilm formation, bacterial adhesion and host response on polymeric implants--issues and prevention. *Biomed Mater* **2008,** *3* (3), 034003.

8. Magill, S. S.; Edwards, J. R.; Bamberg, W.; Beldavs, Z. G.; Dumyati, G.; Kainer, M. A.; Lynfield, R.; Maloney, M.; McAllister-Hollod, L.; Nadle, J.; Ray, S. M.; Thompson, D. L.; Wilson, L. E.; Fridkin, S. K., Multistate Point-Prevalence Survey of Health Care–Associated Infections. *The New England journal of medicine* **2014,** *370* (13), 1198-1208.

9. Kenawy, E.-R.; Worley, S. D.; Broughton, R., The Chemistry and Applications of Antimicrobial Polymers: A State-of-the-Art Review. *Biomacromolecules* **2007,** *8* (5), 1359-1384.

10. Lutchmiah, K.; Verliefde, A. R. D.; Roest, K.; Rietveld, L. C.; Cornelissen, E. R., Forward osmosis for application in wastewater treatment: A review. *Water Research* **2014,** *58*, 179-197.

11. Chun, Y.; Mulcahy, D.; Zou, L.; Kim, I. S., A Short Review of Membrane Fouling in Forward Osmosis Processes. *Membranes* **2017,** *7* (2), 30.

12. Indrani, B.; C., P. R.; S., K. R., Antifouling Coatings: Recent Developments in the Design of Surfaces That Prevent Fouling by Proteins, Bacteria, and Marine Organisms. *Advanced Materials* **2011,** *23* (6), 690-718.

13. Santos, M.; Fonseca, A.; Mendonça, P.; Branco, R.; Serra, A.; Morais, P.; Coelho, J., Recent Developments in Antimicrobial Polymers: A Review. *Materials* **2016,** *9* (7), 599.

14. Muñoz-Bonilla, A.; Fernández-García, M., Polymeric materials with antimicrobial activity. *Progress in Polymer Science* **2012,** *37* (2), 281-339.

15. Francolini, I.; Vuotto, C.; Piozzi, A.; Donelli, G., Antifouling and antimicrobial biomaterials: an overview. *APMIS* **2017,** *125* (4), 392-417.

16. Dang, H.; Lovell, C. R., Microbial Surface Colonization and Biofilm Development in Marine Environments. *Microbiology and Molecular Biology Reviews : MMBR* **2016,** *80* (1), 91-138.

17. Selim, M. S.; Shenashen, M. A.; El-Safty, S. A.; Higazy, S. A.; Selim, M. M.; Isago, H.; Elmarakbi, A., Recent progress in marine foul-release polymeric nanocomposite coatings. *Progress in Materials Science* **2017,** *87*, 1-32.

18. Konai, M. M.; Bhattacharjee, B.; Ghosh, S.; Haldar, J., Recent Progress in Polymer Research to Tackle Infections and Antimicrobial Resistance. *Biomacromolecules* **2018,** *19* (6), 1888-1917.

19. Riga, E. K.; Vöhringer, M.; Widyaya, V. T.; Lienkamp, K., Polymer-Based Surfaces Designed to Reduce Biofilm Formation: From Antimicrobial Polymers to Strategies for Long-Term Applications. *Macromolecular Rapid Communications* **2017,** *38* (20), 1700216.

20. Lam, S. J.; Wong, E. H. H.; Boyer, C.; Qiao, G. G., Antimicrobial polymeric nanoparticles. *Progress in Polymer Science* **2018,** *76*, 40-64.

21. Galvão, C.; Sanches, L.; Mathiazzi, B.; Ribeiro, R.; Petri, D.; Carmona-Ribeiro, A., Antimicrobial Coatings from Hybrid Nanoparticles of Biocompatible and Antimicrobial Polymers. *International Journal of Molecular Sciences* **2018,** *19* (10), 2965.

22. González-Henríquez, C.; Sarabia-Vallejos, M.; Rodríguez Hernandez, J., Antimicrobial Polymers for Additive Manufacturing. *International Journal of Molecular Sciences* **2019,** *20* (5), 1210.

23. Zeng, Q.; Zhu, Y.; Yu, B.; Sun, Y.; Ding, X.; Xu, C.; Wu, Y.-W.; Tang, Z.; Xu, F.-J., Antimicrobial and Antifouling Polymeric Agents for Surface Functionalization of Medical Implants. *Biomacromolecules* **2018,** *19* (7), 2805-2811.

24. Voo, Z. X.; Khan, M.; Xu, Q.; Narayanan, K.; Ng, B. W. J.; Bte Ahmad, R.; Hedrick, J. L.; Yang, Y. Y., Antimicrobial coatings against biofilm formation: the unexpected balance between antifouling and bactericidal behavior. *Polymer Chemistry* **2016,** *7* (3), 656-668.

25. Antizar-Ladislao, B., Environmental levels, toxicity and human exposure to tributyltin (TBT)-contaminated marine environment. A review. *Environment International* **2008,** *34* (2), 292-308.

26. Sonak, S.; Pangam, P.; Giriyan, A.; Hawaldar, K., Implications of the ban on organotins for protection of global coastal and marine ecology. *Journal of Environmental Management* **2009,** *90*, S96-S108.

27. Ponasik, J. A.; Conova, S.; Kinghorn, D.; Kinney, W. A.; Rittschof, D.; Ganem, B., Pseudoceratidine, a marine natural product with antifouling activity: Synthetic and biological studies. *Tetrahedron* **1998,** *54* (25), 6977-6986.

28. Hellio, C.; De La Broise, D.; Dufossé, L.; Le Gal, Y.; Bourgougnon, N., Inhibition of marine bacteria by extracts of macroalgae: potential use for environmentally friendly antifouling paints. *Marine Environmental Research* **2001,** *52* (3), 231-247.

29. Wang, K.-L.; Wu, Z.-H.; Wang, Y.; Wang, C.-Y.; Xu, Y., Mini-Review: Antifouling Natural Products from Marine Microorganisms and Their Synthetic Analogs. *Marine Drugs* **2017,** *15* (9), 266.

30. Yebra, D. M.; Kiil, S.; Dam-Johansen, K., Antifouling technology—past, present and future steps towards efficient and environmentally friendly antifouling coatings. *Progress in Organic Coatings* **2004,** *50* (2), 75-104.

31. Davies, B., Natural rubber — Its engineering characteristics. *Materials & Design* **1986,** *7* (2), 68-74.

32. Gillier-Ritoit, S.; Reyx, D.; Campistron, I.; Laguerre, A.; Pal Singh, R., Telechelic cis-1,4-oligoisoprenes through the selective oxidolysis of epoxidized monomer units and polyisoprenic monomer units in cis-1,4-polyisoprenes. *Journal of Applied Polymer Science* **2003,** *87* (1), 42-46.

33. Sadaka, F.; Campistron, I.; Laguerre, A.; Pilard, J.-F., Controlled chemical degradation of natural rubber using periodic acid: Application for recycling waste tyre rubber. *Polymer Degradation and Stability* **2012,** *97* (5), 816-828.

34. Tran, T. N.; Nourry, A.; Brotons, G.; Pasetto, P., Antibacterial activity of natural rubber based coatings containing a new guanidinium-monomer as active agent. *Progress in Organic Coatings* **2019,** *128*, 196-209.

35. Todd, J. S.; Zimmerman, R. C.; Crews, P.; Alberte, R. S., The antifouling activity of natural and synthetic phenol acid sulphate esters. *Phytochemistry* **1993,** *34* (2), 401-404.

36. Villa, F.; Albanese, D.; Giussani, B.; Stewart, P. S.; Daffonchio, D.; Cappitelli, F., Hindering biofilm formation with zosteric acid. *Biofouling* **2010,** *26* (6), 739-752.

37. Villa, F.; Remelli, W.; Forlani, F.; Vitali, A.; Cappitelli, F., Altered expression level of Escherichia coli proteins in response to treatment with the antifouling agent zosteric acid sodium salt. *Environmental Microbiology* **2012,** *14* (7), 1753-1761.

38. Villa, F.; Pitts, B.; Stewart, P. S.; Giussani, B.; Roncoroni, S.; Albanese, D.; Giordano, C.; Tunesi, M.; Cappitelli, F., Efficacy of Zosteric Acid Sodium Salt on the Yeast Biofilm Model Candida albicans. *Microbial Ecology* **2011,** *62* (3), 584.

39. Barrios, C. A.; Xu, Q.; Cutright, T.; Newby, B.-m. Z., Incorporating zosteric acid into silicone coatings to achieve its slow release while reducing fresh water bacterial attachment. *Colloids and Surfaces B: Biointerfaces* **2005,** *41* (2–3), 83-93.

40. Callow, M. E.; Callow, J. A., Attachment of zoospores of the fouling alga enteromorpha in the presence of zosteric acid. *Biofouling* **1998,** *13* (2), 87-95.

41. Xu, Q.; Barrios, C. A.; Cutright, T.; Newby, B. m. Z., Evaluation of toxicity of capsaicin and zosteric acid and their potential application as antifoulants. *Environmental Toxicology* **2005,** *20* (5), 467-474.

42. Cattò, C.; Dell'Orto, S.; Villa, F.; Villa, S.; Gelain, A.; Vitali, A.; Marzano, V.; Baroni, S.; Forlani, F.; Cappitelli, F., Unravelling the Structural and Molecular Basis Responsible for the Anti-Biofilm Activity of Zosteric Acid. *PLOS ONE* **2015,** *10* (7), e0131519.

43. Chen, L.; Qian, P.-Y., Review on Molecular Mechanisms of Antifouling Compounds: An Update since 2012. *Marine Drugs* **2017,** *15* (9), 264.

44. Kurth, C.; Welling, M.; Pohnert, G., Sulfated phenolic acids from Dasycladales siphonous green algae. *Phytochemistry* **2015,** *117*, 417-423.

45. Kurth, C.; Cavas, L.; Pohnert, G., Sulfation mediates activity of zosteric acid against biofilm formation. *Biofouling* **2015,** *31* (3), 253-263.

46. Guzman, J., Natural Cinnamic Acids, Synthetic Derivatives and Hybrids with Antimicrobial Activity. *Molecules* **2014,** *19* (12), 19292.

47. Jellali, R.; Campistron, I.; Pasetto, P.; Laguerre, A.; Gohier, F.; Hellio, C.; Pilard, J.-F.; Mouget, J.-L., Antifouling activity of novel polyisoprene-based coatings made from photocurable natural rubber derived oligomers. *Progress in Organic Coatings* **2013,** *76* (9), 1203-1214.

48. Badawy, H.; Brunellière, J.; Veryaskina, M.; Brotons, G.; Sablé, S.; Lanneluc, I.; Lambert, K.; Marmey, P.; Milsted, A.; Cutright, T.; Nourry, A.; Mouget, J.-L.; Pasetto, P., Assessing the Antimicrobial Activity of Polyisoprene Based Surfaces. *International Journal of Molecular Sciences* **2015,** *16* (3), 4392.

49. Jellali, R.; Campistron, I.; Laguerre, A.; Lecamp, L.; Pasetto, P.; Bunel, C.; Mouget, J.-L.; Pilard, J.-F., Synthesis and crosslinking kinetic study of epoxidized and acrylated/epoxidized oligoisoprenes: Comparison between cationic and radical photopolymerization. *Journal of Applied Polymer Science* **2013,** *128* (4), 2489-2497.

50. Brandt, D. R.; Pannone, K. M.; Romano, J. J.; Casillas, E. G., The synthetic preparation of naturally-occurring aromatase inhibitors, morachalcone A, isogemichalcone B, and isogemichalcone C. *Tetrahedron* **2013,** *69* (47), 9994-10002.

51. Ouali, S.; Louis, Y.; Germain, P.; Gourdon, R.; Desjardin, V., Leaching and Biodegradation of Darocur 1173 used as a Photo-Initiator in the Production of Photocrosslinked Silicone Acrylates. *Journal of Polymers and the Environment* **2017**.

52. Seidl, B.; Liska, R.; Grabner, G., New photocleavable structures III: Photochemistry and photophysics of pyridinoyl and benzoyl-based photoinitiators. *Journal of Photochemistry and Photobiology A: Chemistry* **2006,** *180* (1), 109-117.

53. Willyard, C., The drug-resistant bacteria that pose the greatest health threats. *Nature* **2017,** *543* (15).

54. Francolini, I.; Piozzi, A.; Donelli, G., Efficacy Evaluation of Antimicrobial Drug-Releasing Polymer Matrices. In *Microbial Biofilms: Methods and Protocols*, Donelli, G., Ed. Springer New York: New York, NY, 2014; pp 215-225.

55. Peng, S.; Zhang, B.; Meng, X.; Yao, J.; Fang, J., Synthesis of Piperlongumine Analogues and Discovery of Nuclear Factor Erythroid 2-Related Factor 2 (Nrf2) Activators as Potential Neuroprotective Agents. *Journal of Medicinal Chemistry* **2015,** *58* (13), 5242-5255.

56. Li, X.; Sheng, J.; Huang, G.; Ma, R.; Yin, F.; Song, D.; Zhao, C.; Ma, S., Design, synthesis and antibacterial activity of cinnamaldehyde derivatives as inhibitors of the bacterial cell division protein FtsZ. *European Journal of Medicinal Chemistry* **2015,** *97*, 32-41.

57. Nishikiwa, H. Preparation of cinnamic acids, Patent Jpn, Kokai Tokkyo Koho, 2002030030. 2002.

58. Jellali, R.; Campistron, I.; Laguerre, A.; Pasetto, P.; Lecamp, L.; Bunel, C.; Mouget, J.-L.; Pilard, J.-F., Synthesis of new photocurable oligoisoprenes and kinetic studies of their radical photopolymerization. *Journal of Applied Polymer Science* **2013,** *127* (2), 1359-1368.

59. Badawy, H. T.; Pasetto, P.; Mouget, J. L.; Pilard, J. F.; Cutright, T. J.; Milsted, A., Bacterial adhesion and growth reduction by novel rubber-derived oligomers. *Biochem Biophys Res Commun* **2013,** *438* (4), 691-6.

60. Decker, C.; Jenkins, A. D., Kinetic approach of oxygen inhibition in ultraviolet- and laser-induced polymerizations. *Macromolecules* **1985,** *18* (6), 1241-1244.

61. Biswal, D.; Hilt, J. Z., Analysis of Oxygen Inhibition in Photopolymerizations of Hydrogel Micropatterns Using FTIR Imaging. *Macromolecules* **2009,** *42* (4), 973-979.

62. Swislocka, R.; Kowczyk-Sadowy, M.; Kalinowska, M.; Lewandowski, W., Spectroscopic (FT-IR, FT-Raman, 1H and 13C NMR) and theoretical studies of p-coumaric acid and alkali metal p-coumarates. *Spectroscopy* **2012,** *27* (1).

63. Minoura, Y.; Yasumoto, N.; Ishii, T., The effect of phenol and cresols on the polymerization of styrene. *Die Makromolekulare Chemie* **1964,** *71* (1), 159-172.

64. Fujisawa, S.; Kadoma, Y., Effect of phenolic compounds on the polymerization of methyl methacrylate. *Dental Materials* **1992,** *8* (5), 324-326.

65. Bird, R. A.; Russell, K. E., The effect of phenols on the polymerization of vinyl acetate. *Canadian Journal of Chemistry* **1965,** *43* (7), 2124-2125.

66. Sathish, M.; Meenakshi, G.; Xavier, S.; Sebastian, S., *Conformational Stability, TGA, and Molecular Docking Investigations of p-Coumaric Acid with Special Relevance to Anti-Cancer and Antibacterial Activity*. 2017; Vol. 131, p 1512-1518.

67. Ouimet, M. A.; Stebbins, N. D.; Uhrich, K. E., Biodegradable Coumaric Acid-based Poly(anhydride-ester) Synthesis and Subsequent Controlled Release. *Macromolecular rapid communications* **2013,** *34* (15), 1231-1236.

68. BASF Darocur 1173 Safety Data sheet, http://www.smfl.rit.edu/pdf/msds/sds_darocur_1173.pdf.

69. Barber, M. S.; McConnell, V. S.; DeCaux, B. S., Antimicrobial intermediates of the general phenylpropanoid and lignin specific pathways. *Phytochemistry* **2000,** *54* (1), 53-56.

70. Lou, Z.; Wang, H.; Rao, S.; Sun, J.; Ma, C.; Li, J., p-Coumaric acid kills bacteria through dual damage mechanisms. *Food Control* **2012,** *25* (2), 550-554.

71. Lejars, M.; Margaillan, A.; Bressy, C., Fouling Release Coatings: A Nontoxic Alternative to Biocidal Antifouling Coatings. *Chemical Reviews* **2012,** *112* (8), 4347-4390.

Graphical abstract